Mapping functional diversity using individual tree-based morphological and physiological traits in a subtropical forest

Zheng, Zhaoju ; Zeng, Yuan ; Schneider, Fabian D ; Zhao, Yujin ; Zhao, Dan ; Schmid, Bernhard ; Schaepman, Michael E ; Morsdorf, Felix

Abstract: Functional diversity (FD) provides a link between biodiversity and ecosystem functioning, summarizing inter- and intra-specific variation of functional traits. However, quantifying plant traits and FD consistently and cost-effectively across large and heterogeneous forest areas is challenging with traditional field sampling. Airborne light detection and ranging (LiDAR) and imaging spectroscopy provide spatially explicit data, which allow mapping of selected forest traits and FD at different spatial scales. We develop an individual tree-based method to measure forest FD from tree neighborhoods to whole forests, and demonstrate the approach by mapping functional traits of over one million trees in a subtropical forest in China. We retrieved canopy morphological traits (95th quantile height, leaf area index and foliage height diversity) and physiological traits (proxies of nitrogen, carotenoids and specific leaf area) for each individual canopy tree crown from LiDAR and imaging spectroscopy data, respectively. Based on the multivariate trait space spanned by the six trait axes and filled by measured tree individuals, we mapped forest FD as richness, divergence and evenness, and explored spatial patterns of FD as well as FD–area and FD–tree number relationships. The results show that LiDAR-derived morphological traits and spectral indices of physiological traits are consistent with field measurements and show weak correlations between each other at individual tree level. Morphological functional richness follows a hump-shaped pattern along the elevational gradient of 984–1805 m, with maximum values at elevations around 1450 m, while high physiological functional richness occurs at medium and high elevations. At an ecosystem scale of 30 × 30 m, morphological richness increases continuously with tree density, but physiological richness decreases again at very high densities. Moreover, functional richness shows a logarithmic relationship with increasing area or number of individual trees, and local trait convergence is predominant in our study area. We demonstrate the ability to quantify FD using morphological and physiological traits by remote sensing, which provides a pathway to conduct individual-level trait-based ecology with wall-to-wall data.

DOI: https://doi.org/10.1016/j.rse.2020.112170

Originally published at:
Zheng, Zhaoju; Zeng, Yuan; Schneider, Fabian D; Zhao, Yujin; Zhao, Dan; Schmid, Bernhard; Schaepman, Michael E; Morsdorf, Felix (2021). Mapping functional diversity using individual tree-based morphological and physiological traits in a subtropical forest. Remote Sensing of Environment, 252:112170.
DOI: https://doi.org/10.1016/j.rse.2020.112170

Remote Sensing of Environment 252 (2021) 112170

Contents lists available at ScienceDirect

Remote Sensing of Environment

journal homepage: www.elsevier.com/locate/rse

Mapping functional diversity using individual tree-based morphological and physiological traits in a subtropical forest

Zhaoju Zheng [a,b], Yuan Zeng [b,c,*], Fabian D. Schneider [d], Yujin Zhao [e], Dan Zhao [b], Bernhard Schmid [a], Michael E. Schaepman [a], Felix Morsdorf [a]

[a] Remote Sensing Laboratories, Department of Geography, University of Zurich, Zurich CH-8057, Switzerland
[b] State Key Laboratory of Remote Sensing Science, Aerospace Information Research Institute, Chinese Academy of Sciences, Beijing 100101, China
[c] University of Chinese Academy of Sciences, Beijing 100049, China
[d] Jet Propulsion Laboratory, California Institute of Technology, Pasadena, CA 91109, USA
[e] State Key Laboratory of Vegetation and Environmental Change, Institute of Botany, Chinese Academy of Sciences, Beijing 100093, China

ARTICLE INFO

Keywords:
LiDAR
Imaging spectroscopy
Forest diversity
Functional traits
Individual tree-based approach
Scaling

ABSTRACT

Functional diversity (FD) provides a link between biodiversity and ecosystem functioning, summarizing inter- and intra-specific variation of functional traits. However, quantifying plant traits and FD consistently and cost-effectively across large and heterogeneous forest areas is challenging with traditional field sampling. Airborne light detection and ranging (LiDAR) and imaging spectroscopy provide spatially explicit data, which allow mapping of selected forest traits and FD at different spatial scales. We develop an individual tree-based method to measure forest FD from tree neighborhoods to whole forests, and demonstrate the approach by mapping functional traits of over one million trees in a subtropical forest in China. We retrieved canopy morphological traits (95th quantile height, leaf area index and foliage height diversity) and physiological traits (proxies of nitrogen, carotenoids and specific leaf area) for each individual canopy tree crown from LiDAR and imaging spectroscopy data, respectively. Based on the multivariate trait space spanned by the six trait axes and filled by measured tree individuals, we mapped forest FD as richness, divergence and evenness, and explored spatial patterns of FD as well as FD–area and FD–tree number relationships. The results show that LiDAR-derived morphological traits and spectral indices of physiological traits are consistent with field measurements and show weak correlations between each other at individual tree level. Morphological functional richness follows a hump-shaped pattern along the elevational gradient of 984–1805 m, with maximum values at elevations around 1450 m, while high physiological functional richness occurs at medium and high elevations. At an ecosystem scale of 30 × 30 m, morphological richness increases continuously with tree density, but physiological richness decreases again at very high densities. Moreover, functional richness shows a logarithmic relationship with increasing area or number of individual trees, and local trait convergence is predominant in our study area. We demonstrate the ability to quantify FD using morphological and physiological traits by remote sensing, which provides a pathway to conduct individual-level trait-based ecology with wall-to-wall data.

1. Introduction

Forests are a vital part of the terrestrial biosphere, providing not only valuable ecosystem goods and services but also supporting a vast biodiversity of organisms (Liang et al., 2016). However, the biodiversity of forests is facing unprecedented decline globally due to human activity and climate change, which might in turn substantially diminish the services that ecosystem provides to humanity (Díaz et al., 2006; Fang et al., 2012). The biodiversity of an area is comprised of at least three components — composition, structure and function — evaluated at all levels of the biological hierarchy, from genes to ecoregions (Noss, 1990). Previous biodiversity inventory has mainly been based on compositional and structural features (especially at species level), while functional features remained underexplored for a long time, but they now receive increasing attention with the emergence of functional biogeography (Ammer et al., 2018; Kattge et al., 2020; McGill et al., 2006; Violle et al.,

* Corresponding author at: State Key Laboratory of Remote Sensing Science, Aerospace Information Research Institute, Chinese Academy of Sciences, Beijing 100101, China.
E-mail address: zengyuan@radi.ac.cn (Y. Zeng).

https://doi.org/10.1016/j.rse.2020.112170
Received 30 April 2020; Received in revised form 25 October 2020; Accepted 27 October 2020
Available online 11 November 2020

2014).

Functional diversity (FD), referred to as the value, range and distribution of functional traits of the organisms in a given ecosystem (Díaz and Cabido, 2001; Petchey and Gaston, 2006), is a major component of biodiversity. It can help to predict ecosystem functioning by accounting for both inter- and intra-specific variability and functional redundancy (Duffy et al., 2017; Hooper et al., 2005; Ruiz-Benito et al., 2014). The methods for measuring FD have turned from taxonomy-based categorical classifications of functional traits (e.g., functional groups) to taxonomy-independent continuous multi-trait approaches using variance- or distance-based metrics (Laliberté and Legendre, 2010; Petchey and Gaston, 2002; Swenson et al., 2012; Villéger et al., 2008; Violle et al., 2014; Walker, 1992). Different multivariate FD indices, e.g., functional richness, divergence and evenness, represent different aspects of multivariate trait distributions and can thus be used complementarily (Ahmed et al., 2019; Carmona et al., 2016; Mason et al., 2005; Schneider et al., 2017; Villéger et al., 2008). A critical point in developing predictive measures of FD is the choice of functional traits (Petchey and Gaston, 2006). Ecologically meaningful functional traits representing morphological and physiological characteristics of organisms are critical indicators for FD monitoring (Díaz et al., 2016; Homolová et al., 2013; Petchey and Gaston, 2006; Violle et al., 2007). For example, morphological traits such as tree height and multi-layered foliage structure could affect light availability, individual tree growth, ecosystem productivity and habitat for canopy dwelling organisms (Moles et al., 2009; Ishii et al., 2004). Leaf area index (LAI) as a measure of leaf surface available for photosynthesis and transpiration, plays a key role in the energy fluxes between the atmosphere and vegetation (Chen et al., 1997). Physiological traits such as leaf nitrogen and carotenoids are closely related to leaf photosynthesis, metabolism and photoprotection (Jetz et al., 2016; Asner et al., 2015). Specific leaf area (SLA, the inverse of leaf mass per area) relates the area of light interception to leaf biomass, reflecting a trade-off between construction cost and leaf lifespan (Díaz et al., 2016). Functional traits directly link to organismal functions (growth, reproduction and survival) and ecosystem functioning, and vary between and within species, across environmental gradients (Bongers et al., 2020; Fyllas et al., 2017; McGill et al., 2006; Messier et al., 2017).

However, field measurements of plant traits are limited to relatively small and unevenly distributed sampling areas due to the complexity and costs (time, labor and expense) of traditional in-situ measurements. Although the availability of trait datasets is constantly improving (Kattge et al., 2020), data from different sources might suffer from bias due to operators' subjective interpretation or different measurement methods (Kattge et al., 2011). More importantly, these trait datasets depend on taxonomic information, which is not always available (i.e. without knowledge about species identities of individuals, traits cannot be extracted from the available sources). Many trait records use the average trait values of collected samples for each species, assuming that all individuals of a species in a region share the same trait value (Swenson and Weiser, 2010). This fails to describe trait variation between individuals within species, potentially due to genetic or environmental differences. Therefore, measuring traits consistently over large areas with high accuracy is an urgent need (Jetz et al., 2016; Marconi et al., 2019b; Reich, 2005).

Remote sensing combined with in-situ data provides a realistic and efficient way to quantify plant traits at large scales. Existing remote sensing approaches to assess forest morphological traits (or canopy structure in general) are mainly based on statistical models, physical models, or combinations thereof. Statistical approaches depend on in-situ collected structural variables and site-specific model calibrations. Physical models (often implemented as geometric optical models), consider forest stands as a combination of approximated geometrical shapes of tree crowns with corresponding shadows and background (Li and Strahler, 1985). In the past few decades, these approaches have been applied to estimate plant morphological traits (e.g., height, canopy cover, LAI) with optical sensors such as Landsat, Sentinel-2 and MODIS as well as high-spatial-resolution Quickbird and high-spectral-resolution EO-1 Hyperion (Garrigues et al., 2008; Korhonen et al., 2017; Ma et al., 2019; Zeng et al., 2008b, 2009). However, these two-dimensional optical images have a limited capability to adequately capture detailed canopy structure information. Airborne light detection and ranging (LiDAR) data provide a quantitative, three-dimensional view of the vegetation on different scales, being extensively used to derive canopy structural variables with high accuracy (Ferreira et al., 2018; Lefsky et al., 2002; Marconi et al., 2019a; Morsdorf et al., 2004, 2018; Noordermeer et al., 2019; Schneider et al., 2014). Furthermore, advances in LiDAR measurement technology have enabled the accurate extraction of tree-level information (Kaartinen et al., 2012; Morsdorf et al., 2004; Popescu and Wynne, 2004; Seidel et al., 2019; Wang et al., 2016a), making it possible to conduct individual tree-based ecology at large scales with spatially explicit data (Duncanson and Dubayah, 2018). Morphological traits extracted from individual canopy trees could be used to assess how tree assemblages fill the trait space in a specific community, which is essential to understand community assembly processes (Clark et al., 2011; Liu et al., 2016).

Imaging spectroscopy (also called hyperspectral remote sensing) shows potential for ecologically relevant forest monitoring by providing full-spectral information sensitive to many functional traits (Asner and Martin, 2009, 2016; Gamon et al., 2019; Schaepman et al., 2009, 2015; Ustin et al., 2009). Widely-used physiological traits (e.g., chlorophyll, carotenoids, nitrogen, water content) have been successfully derived from imaging spectroscopy data at the leaf or canopy level across multiple biomes based on empirical or physical models (Casas et al., 2014; Féret et al., 2011, 2019; Hill et al., 2019; Koetz et al., 2007; Malenovský et al., 2013; Serbin et al., 2014; Singh et al., 2015; Verrelst et al., 2015; Wang et al., 2016b, 2020). Most existing remotely sensed physiological trait estimations, however, are computed at the pixel level, which might mix several individuals or parts of individuals depending on the spatial resolution (Ma et al., 2019; Serbin et al., 2015; Wang and Gamon, 2019). Advanced remote sensing methods such as individual tree detection from LiDAR or high-resolution orthophotos allow for estimating physiological traits or proxies of traits at the level of individual trees, thus avoiding mixing of different biological entities (Chadwick and Asner, 2016; Martin et al., 2018; Zhao et al., 2018). Obviously, tree inventory research based on individual-level functional traits can better capture ecological processes in forest communities than methods using species-mean traits (Paine et al., 2011). In forest communities, individual trees interact with their neighbors as well as their abiotic and biotic environment. They hence vary substantially in their traits and performance (Harper, 1977). As a consequence, it can also be expected that individual-based FD indices show stronger links to ecosystem functioning than do pixel-based indices (Yang et al., 2018). This should not only apply to morphological traits but also to physiological traits, which can contribute critical information for predictive ecosystem models and may show particularly strong relations between FD and ecosystem functioning (Cadotte et al., 2011; Mouchet et al., 2010).

Recent large-scale FD studies used dynamic global vegetation models (DGVMs) based on climate and soil data to predict FD patterns with coarse resolutions, for example, the functional dispersion and range in plant traits (Sakschewski et al., 2015; Thonicke et al., 2020). At the continental scale, Ma et al. (2019) applied partial least squares regression (PLSR) linking Sentinel-2 multispectral reflectance variables with functional dispersion calculated from field surveys using species-level foliar and whole-plant traits on 117 plots in six European forests. Spaceborne measurements can be applied to a larger geographic extent, but so far it has been difficult to extract relevant plant traits directly from the spectral data for individual trees rather than by correlation with ground-based data from vegetation plots potentially containing multiple species (Ma et al., 2020). Spectroscopic trait measurements combined with LiDAR-derived structural features at individual tree level hold great promise to enhance the ecological interpretation of spectral

imagery (Ewald et al., 2018a, 2018b; Jetz et al., 2016; Schimel et al., 2019; Ustin and Gamon, 2010).

Previous studies on remote sensing of forest functional diversity with high spatial resolution have focused on pixel-based approaches. For example, Schneider et al. (2017) developed a pixel-based, spatially continuous method to map FD across a temperate mixed forest based on morphological and physiological traits. Similarly, Durán et al. (2019) estimated single- and multi-trait metrics of FD in tropical forests along an Amazon-Andes elevation gradient, whereas Asner et al. (2017) derived FD from forest functional classes in the same study area. Furthermore, Durán et al. (2019) showed that pixel-based functional richness was positively linked to ecosystem productivity. However, although FD has received increasing attention, the pixel-based approaches still look at vegetation canopies rather than individual trees; the potential of individual-based FD monitoring from remote sensing remains to be demonstrated and the scale-dependency of individual-based FD is not yet clear (Karadimou et al., 2016; Smith et al., 2013). Moreover, tree density is an important variable related to diversity (Magurran, 2004), but can not be assessed with pixel-based approaches. Previous research has shown that morphological and physiological traits can significantly differ between trees in low density (weak competition) and high density (strong competition) stands (Juchheim et al., 2020; Pommerening and Grabarnik, 2019; Pretzsch and Biber, 2005, 2016) or forests with low and high diversity (Bongers et al., 2020). Likewise, tree density and forest diversity may interact, because diversity reduces competition between individuals due to niche differentiation and facilitation and allows more individuals to occupy a unit of area (Baruffol et al., 2013; Paquette and Messier, 2011). Most knowledge on these relationships stems from studies based on experimental or inventory plots, but the relationships between FD and tree density in spatially continuous forests remain unclear.

Therefore, the primary objective of this paper is to develop a new method for mapping forest FD based on remotely sensed individual-tree functional traits. To achieve this, we (1) quantified the distribution of functional traits by retrieving morphological and physiological traits for more than one million individual trees from airborne LiDAR and imaging spectroscopy data and validated them against in-situ data; (2) mapped forest FD maximizing the representation of the variation between individuals by calculating multivariate FD indices across elevation gradients using a moving window approach; and (3) further explored the relationship between tree density and forest FD at areas of 30 × 30 m and analyzed FD–area and FD–tree number relationships. Our study demonstrates that FD can be quantified at different scales based on individual-level traits by airborne remote sensing, providing a pathway to address trait-based ecology with wall-to-wall data across environmental gradients.

2. Materials

2.1. Study area

This study was performed at the Shennongjia National Forest Natural Reserve in Xingshan county, Hubei province of China with an area of about 11 × 14 km covered by an airborne campaign (see Section 2.2 for details). A region called Longmenhe (3.5 × 3 km, center coordinates: 31° 20′ N, 110° 29′ E) located on the south slope of Mt. Shennongjia with old-growth, secondary and planted forests was selected for method development and a scaling study (Fig. 1). The climate of this area is a transitional type between the north-subtropical and the warm-temperate moist monsoon. The mean annual precipitation is ca. 1380 mm and the mean annual temperature is ca. 10.2 °C based on the meteorological records of 2001–2012 from the National Field Research Station for Forest Ecosystem in Shennongjia located at 1290 m a.s.l. The dominant soils are Mountain Yellow Cinnamon and Brown Earth (Zeng et al., 2008a).

The Shennongjia National Forest Natural Reserve is characterized by subtropical evergreen and deciduous broad-leaved mixed forest and is a globally important biodiversity hotspot (Myers et al., 2000). For the Longmenhe region we recorded more than 150 tree species in our field measurements, representing most of the dominant species in the Shennongjia National Forest Natural Reserve. Forest type varies along the elevational gradient from (i) evergreen broad-leaved forests (dominant species are *Cyclobalanopsis multinervis*, *Cyclobalanopsis oxyodon* and *Lithocarpus glaber*) at low elevations to (ii) mixed evergreen and deciduous broad-leaved forests (dominant deciduous species include *Fagus engleriana*, *Betula luminifera*, *Platycarya strobilacea*, *Quercus serrata*,

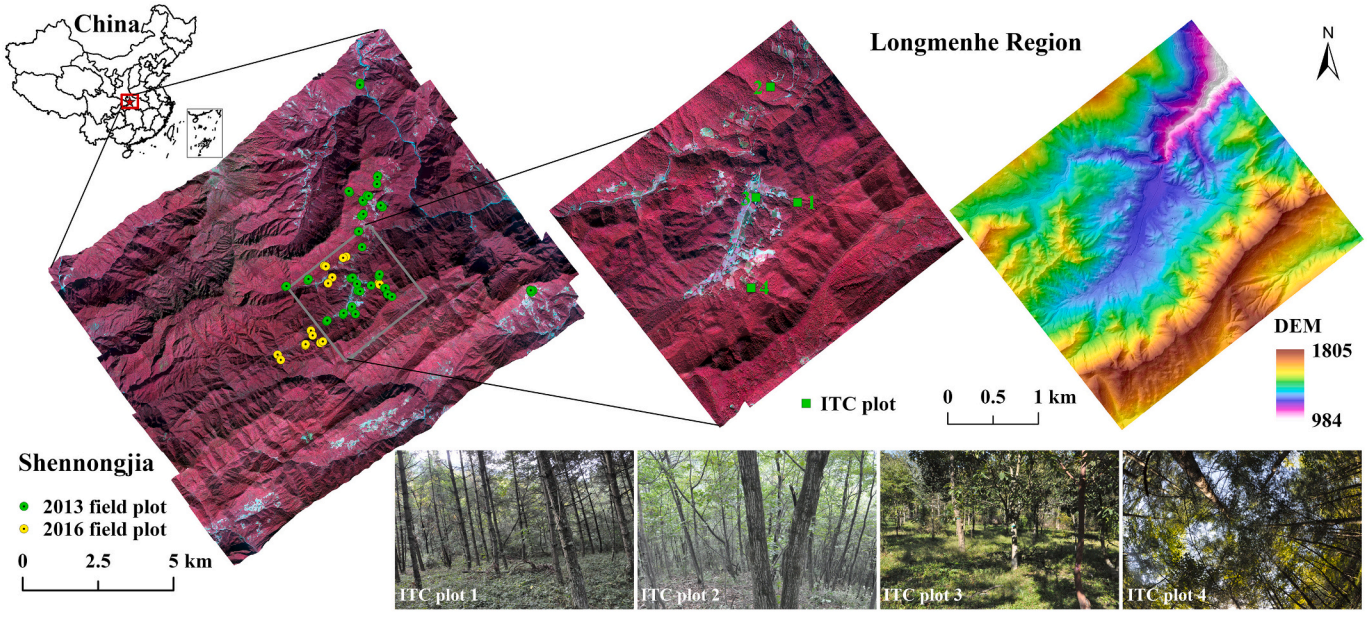

Fig. 1. The Shennongjia National Forest Natural Reserve (left) and Longmenhe region (middle) with imaging spectroscopy data acquired using the Pushbroom Hyperspectral Imager-3 (PHI-3, Red: 812 nm, Green: 655 nm, Blue: 550 nm) and LiDAR-derived digital elevation model (DEM) (right). The circles indicate the locations of field-measured sample plots in 2013 and 2016. The squares indicate the locations of individual tree (ITC) validation plots. Four photographs of these ITC plots are shown below. (For interpretation of the references to color in this figure legend, the reader is referred to the web version of this article.)

Quercus aliena and *Sorbus folgneri*), to (iii) mixed coniferous and broad-leaved forests and to (iv) coniferous forests (dominant species are *Pinus massoniana*, *Larix kaempferi* and *Cunninghamia lanceolata*) at high elevations (Pei et al., 2018; UNESCO World Heritage Centre, 2016; Xu et al., 2017). In the 1970s, this region became an important wood-cutting area, causing severe destruction to the biological resources. But due to inconvenient transportation, 60% of the primeval forest survived. Deforestation was forbidden, to allow vegetation recovery, when the reserve was established in 1982 (Ge et al., 1997).

2.2. Airborne LiDAR & imaging spectroscopy data

The LiDAR data acquisition was conducted above the Shennongjia study area in October 2013 using a Leica ALS70-HP laser scanner (Leica Geosystems AG, Heerbrugg, Switzerland) mounted on a Yun-5 turboprop aircraft. The laser system emitted pulses with a wavelength of 1064 nm. The maximum scan angle of ±17° from nadir and about 25% flight strip overlap led to an average point density of more than 4 points/m^2. The LiDAR data were co-registered, classified to ground and non-ground returns using Terrasolid software (Terrasolid, Helsinki, Finland) by the vendor (SHHANGYAO Inc., Shanghai, China) and projected to the Universal Transverse Mercator (UTM) Zone 49 N/WGS-84 coordinate system. The positional accuracy of the LiDAR point clouds was <0.3 m in horizontal and <0.1 m in vertical direction. A gap-filled Canopy Height Model (CHM) (Zhao et al., 2013) was used to extract individual tree crowns, and elevation-normalized LiDAR point clouds were used to derive the morphological traits as described below (Section 3.3).

Twenty-one imaging spectroscopy scenes were acquired on 11 October and 13 October 2013 from 10:30 to 13:30 local time under cloudless conditions using the Pushbroom Hyperspectral Imager-3 (PHI-3, designed by Shanghai Institute of Technical Physics, Chinese Academy of Sciences). The PHI-3 instrument was mounted on a Yun-5 turboprop aircraft that flew over the study area at 1500 m above ground level, resulting in a ground resolution of 1 m. It contained two sensors recording the 440–1000 nm and 1000–2500 nm spectral ranges with 189 and 256 bands, respectively. The spectral resolution (full width at half maximum) varied depending on wavelength, averaging 3 nm for the visible and near-infrared range and 5 nm for the near-infrared and short-wave infrared range. The pre-processing of the imaging spectroscopy data was described in detail in Zhao et al. (2018). The reflectance images were used to derive the physiological traits as described below (Section 3.3).

2.3. Field measurements

We collected field measurements of 46 square sample plots (30 × 30 m) in the Shennongjia study area in September and October 2013. We recorded the four corner coordinate pairs of each plot using a Trimble GeoXH 3000 handheld GPS and combined the measurements from base station for differential correction. For each plot, we measured the tree height, diameter at breast height (DBH), crown base height, crown diameters and species for all individual trees with DBH ≥ 5 cm. We additionally measured the exact location of each tree in four of the sample plots by integrating the Real-Time Kinematic (RTK) GPS/GLONASS System with a total station for validating the individual tree crown detection accuracy. We also selected 19 individual canopy trees in the study area and took upward-oriented hemispherical photographs using a Nikon camera with a fish-eye lens and bubble level attachment, and then used Can-Eye v6.36 software to estimate the LAI of these trees.

In addition, we collected sunlit top-of-canopy leaves from 31 canopy trees with GPS locations (for each tree 3 samples) across 13 plots in the Shennongjia study area in September of 2016. The leaf carotenoid content, nitrogen concentration and SLA of these samples were measured in the laboratory, following the method described in Zhao et al. (2016). These in-situ traits (Table S1) were used to validate the physiological traits obtained from imaging spectroscopy data.

3. Methods

3.1. Overview of methodology

A workflow of the major methods utilized in this study is illustrated in Fig. 2. First, we performed an individual tree crown (ITC) detection from the airborne LiDAR data. For each ITC, we retrieved three morphological traits and three physiological traits from the airborne LiDAR and imaging spectroscopy data, respectively. Then, we developed a spatially complete individual tree-based method to map three aspects of forest FD, functional richness, divergence and evenness, at different scales and analyzed their spatial patterns. Furthermore, we tested whether FD correlated with tree density at 30 × 30 m ecosystem scale. An area of 30 × 30 m has been identified as a relevant ecosystem scale in Chinese subtropical forests nearby (Liu et al., 2016). Finally, we analyzed FD–area and FD–tree number relationships and explored the scale dependency of forest FD in the Longmenhe region.

3.2. Individual tree crown detection

We used a morphological crown control-based watershed algorithm for ITC segmentation (Chen et al., 2006; Zhao et al., 2013, 2014), which performed well when applied on the same data in a similar context (Zhao et al., 2018). Firstly, a Laplacian operator and a morphological closing operator with thresholds were used to fill pits of the LiDAR-derived CHM and determine the crown areas. Then a local maxima algorithm was adopted to identify potential treetops in the crown areas. Two watershed transformations combined with a reconstruction operation were applied to delineate the tree crowns and restrain over-segmentation problems. Finally, the crown outlines were adaptively optimized based on a morphological opening operator on each

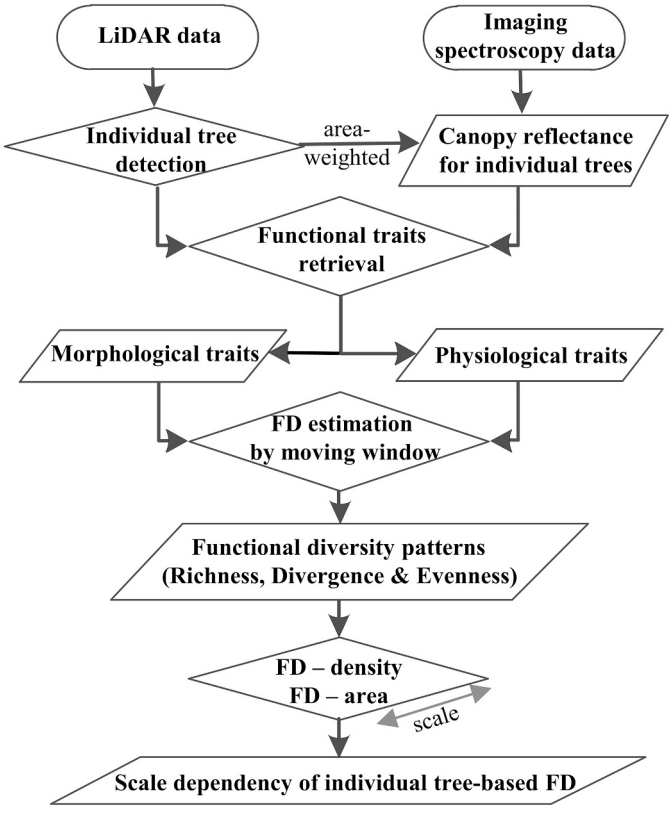

Fig. 2. Flowchart of the processing steps for measuring forest FD using remote sensing data.

watershed segment. The position of treetops, the crown polygons and the tree height (>3 m) were used in the subsequent estimation of functional traits and FD.

As the field-measured stem positions were not always at the same horizontal locations of the treetops, we evaluated the LiDAR-derived ITCs (match, omission and commission) with field-measured individual tree positions using distance and tree height as matching criteria. We also calculated the match rates for five DBH groups (quintiles) to assess the ITC detection capability for both large and small trees.

3.3. Functional traits retrieval

A set of individual-tree morphological and physiological traits were selected and retrieved from airborne LiDAR and imaging spectroscopy data, respectively. A basic principle for trait selection is that they should indicate essential functions related to the ecosystem processes or functioning one wants to investigate (Mason and Mouillot, 2013). In our case, in view of planned analyses about ecosystem carbon cycling and diversity–productivity relationships of the studied forest, we were particularly interested in traits related to photosynthesis, growth and complementarity in resource use (Huang et al., 2018; Reich, 2012).

For morphological traits, we chose the commonly used 95th quantile height (H_{95}, approximates canopy tree height; the 95th quantile height of LiDAR first returns), leaf area index (LAI, projected leaf and branch area per horizontal ground area; also known as plant area index) and foliage height diversity (FHD, the density and height distribution of canopy layers), describing the vertical height, horizontal openness and internal complexity of canopy structure, respectively (Coops et al., 2016; Fahey et al., 2019; Valbuena et al., 2020). Individual-tree LAI was derived based on the method proposed by Richardson et al. (2009), as shown in Eq. (1):

$$\begin{cases} \mathrm{GF} = \dfrac{n_{ground}}{n_{vegetation} + n_{ground}} \\ \mathrm{LAI} = -cos(\theta) * \dfrac{ln(\mathrm{GF})}{\mathrm{k}} \end{cases} \quad (1)$$

where θ is zenith angle (LiDAR scanning angle), k is the extinction coefficient mainly determined by leaf angle distribution and is simply assumed to be 0.5 (spherical leaf angle) if the vegetation is deemed to follow the spherical leaf angle distribution, and GF is gap fraction, which denotes the fraction of ground returns over total returns. To reduce the effects of increasing scan angle on GF, the LiDAR point clouds were filtered to a maximum scan angle of ±10° before LAI retrieval. FHD was calculated following the Shannon-Wiener index based on LiDAR first returns as Eq. (2):

$$H = -\Sigma p_i \, ln \, p_i, \quad (2)$$

Where p_i is the proportion of horizontal vegetation in the ith layer (3 m vertical interval), namely, the ratio of LiDAR returns in the ith layer to the total returns (Clawges et al., 2008; MacArthur and MacArthur, 1961). We derived the morphological traits for every single tree of the canopy using terrain-corrected point clouds inside the crown polygons. The traits were then linearly rescaled to [0, 1] using a min-max normalization after trimming the upper and lower extremes based on visual inspection of the trait histograms, i.e. 1st to 99.5th percentile for H_{95} and 2nd to 98th percentile for LAI and FHD.

For physiological traits, we chose leaf carotenoids (the relative content of carotenoids per unit leaf area, unit: μg•cm^{-2}), SLA (the ratio of leaf area to dry mass, unit: cm^2•g^{-1}) and leaf nitrogen (the relative concentration of nitrogen per unit leaf mass, unit: %), indicating light utilization and protection, plant growth and longevity as well as photosynthetic and metabolic capacity (Díaz et al., 2016; Jetz et al., 2016; Wright et al., 2004). We selected three hyperspectral vegetation indices (VIs), namely carotenoid reflectance index (CRI, Gitelson et al., 2002) simple ratio index (SR, Jordan, 1969) and normalized difference nitrogen index (NDNI, Serrano et al., 2002), based on the Gini importance of random forest regression (Zhao et al., 2018) to represent the three physiological traits and derived them from imaging spectroscopy data based on the following formulae (Eqs. (3), (4), (5)):

$$\mathrm{CRI} = 1/\mathrm{R}_{510} - 1/\mathrm{R}_{550} \quad (3)$$

$$\mathrm{SR}[705, 750] = \mathrm{R}_{750}/\mathrm{R}_{705} \quad (4)$$

$$\mathrm{NDNI} = [log(1/R_{1520}) - log(1/\mathrm{R}_{1680})]/[log(1/\mathrm{R}_{1520}) + log(1/\mathrm{R}_{1680})] \quad (5)$$

Considering that the retrieval of physiological traits in shaded areas can be severely impacted by noise and an unknown spectral response under diffuse illumination conditions (Nagendra and Rocchini, 2008), only sunlit pixels (threshold based on histogram CRI > 11.92) within each ITC were considered for analysis. Since pixels are not always fully enclosed within tree crown polygons, we calculated the area-weighted mean of these VIs based on the intersection of the pixels with crown polygons as the proxies of physiological traits for each ITC. Then the physiological traits were linearly rescaled to [0, 1] using a min-max normalization after trimming the extremes based on visual inspection of the trait histograms, i.e. 0.5th to 100th percentile for CRI, 5th to 98th percentile for SR and 0.5th to 95th percentile for NDNI.

To compare the canopy reflectance-based estimates of physiological traits with the in-situ individual-tree leaf biochemical measurements in 2016, canopy hyperspectral VIs of the specific individual trees were divided by ITC's LAI to downscale to leaf level (Homolová et al., 2013; Zarco-Tejada et al., 2001). We evaluated the remotely sensed physiological traits with field measurements at leaf level using linear models by calculating the coefficient of determination (R^2) and P-value.

In addition, we calculated Pearson correlations for each pair of normalized traits across all detected trees in the Longmenhe region. Moreover, we generated 1000 bootstrapped trait datasets (1% of the trees) to estimate the significance of the correlations by calculating the confidence interval of trait–trait correlations at 95% level (Flores-Moreno et al., 2019).

3.4. Multivariate functional diversity indices

We calculated multivariate FD indices for the retrieved individual-tree traits, one set for morphological and one set for physiological traits. Each set contained the three multivariate FD indices functional richness (FRic), divergence (FDiv) and evenness (FEve) (see detailed description in Table S2). FRic corresponds to the functional niche occupied by the organisms of a community, while FDiv and FEve describe the distribution of the organisms within the functional trait space (Villéger et al., 2008). At species level, these measures reflect the niche of single species, at community level they reflect the community niche (Salles et al., 2009). High and low FDiv values represent broad and narrow niches, respectively; high values indicating differences between individuals or species and low values indicating similarities between individuals or species. Differences have been hypothesized to indicate limiting similarity constraints and similarities have been hypothesized to be due to environmental filtering (Cornwell et al., 2006; Garnier and Navas, 2012; Spasojevic and Suding, 2012). High FEve means a regular distribution of the traits, while low FEve means clumping or irregular distributions in trait space, potentially indicating under-utilization of resources (Schleuter et al., 2010) or the absence of corresponding conditions in the environment.

We calculated and mapped the FD indices of the Longmenhe region based on a 30 × 30 m grid using the functional traits of individual trees in every grid cell. Compared with FD measurements based on species presence/absence data or species abundance weighting (Mendes et al., 2015), our approach does not use species, i.e. combines inter- and intraspecific trait variation, and implicitly uses abundance weighting because every tree provides trait measurements and has the same weight in the analysis. FRic was calculated as the convex hull volume of the

trees considered to constitute the community, here referred to as neighborhood, in multidimensional functional trait space (convhull, Matlab). Neighborhood was either defined as a given area or as a given number of trees and the corresponding analysis referred to as area- or number-based analysis. FDiv and FEve were calculated in Matlab based on Villéger et al. (2008) and Schneider et al. (2017). Considering the density effect for diversity in ecological studies (Baruffol et al., 2013; Harper, 1977), we also explored the relationship between area-based FRic and tree density at 30 × 30 m ecosystem scale.

3.5. FD–area and FD–tree number relationships

To analyze the area-based scale-dependency, we used a moving window approach (window size = grid size = 3 × 3 m) to calculate the FD indices for the whole study area with varying neighborhoods. Since diversity was always measured within a specific geographical unit for the area-based analysis, we calculated the FD indices based on the functional traits of individual trees in a radial neighborhood of the center of the moving window and assigned the FD indices to the corresponding grid cell. The crown diameter was on average 3 m, hence we chose a radial neighborhood with 9 m radius as the smallest area, which typically would include approximately 36 trees with average crown diameter. To test how FD changed with area (spatial extent), we calculated the FD indices for an increasing neighborhood ranging from 9 to 504 m radius with a step of 7.5 m (resulting in 67 different neighborhood calculations). Then we averaged the FD index values of all forest grid cells (inside a 500 m buffer of the study boundary) for each neighborhood extent to derive FD–area curves. We fitted power-law and logarithmic functions to the observed relationships between morphological and physiological FRic indices and area. In addition, we randomized the locations of trees and calculated FRic based on a null model of spatially randomly distributed trees (rand, Matlab), to test if the functional traits followed a random distribution, or whether there was trait convergence or divergence within neighborhoods. Each tree kept its values for the morphological and physiological traits as in the non-randomized dataset.

To analyze the number-based scale-dependency, we generated 1000 random points within 500 m of the border and selected the points with more than 10,000 trees within a buffer of 250 m radius as central points to avoid non-forested areas. Then we calculated FD for changing tree numbers ranging from 9 to 10,000 with a step function of 100 trees by adding the closest trees (to the central point) to the neighborhood. We averaged FD index values of the central points for each neighborhood to derive FD–tree number curves. We also fitted power-law and logarithmic functions to the observed relationships between morphological and physiological FRic indices and tree number.

4. Results

4.1. Individual tree crown detection

The field-measured positions and tree heights of ITCs in four detailed-measured plots were used to evaluate the individual tree detection results. The number of reference trees, correctly matched, missed (omission), and extra trees (commission) are shown in Fig. 3. Totally 335 trees were detected from LiDAR data and 311 trees were correctly matched with the 373 reference trees in the four plots (83.4%). Under-segmentation because of overlapping tree crowns, understory and multi-stemmed trees were the main causes of the 16.6% omissions error, especially for the two broad-leaved forest plots (Fig. 3; Supp Fig. 1). The detection rates were 87.0%, 90.6% for the coniferous and the conifer-dominated plots (plot 1 and 4), respectively, and 70.5% and 82.4% for the two broad-leaved forest plots (plot 2 and 3, respectively). The unmatched trees also included some over-segmented ITCs due to the presence of more than one potential treetop in larger and rougher canopy parts. Totally 24 extra trees were “detected”, corresponding to a commission error across all four plots of 7.2%.

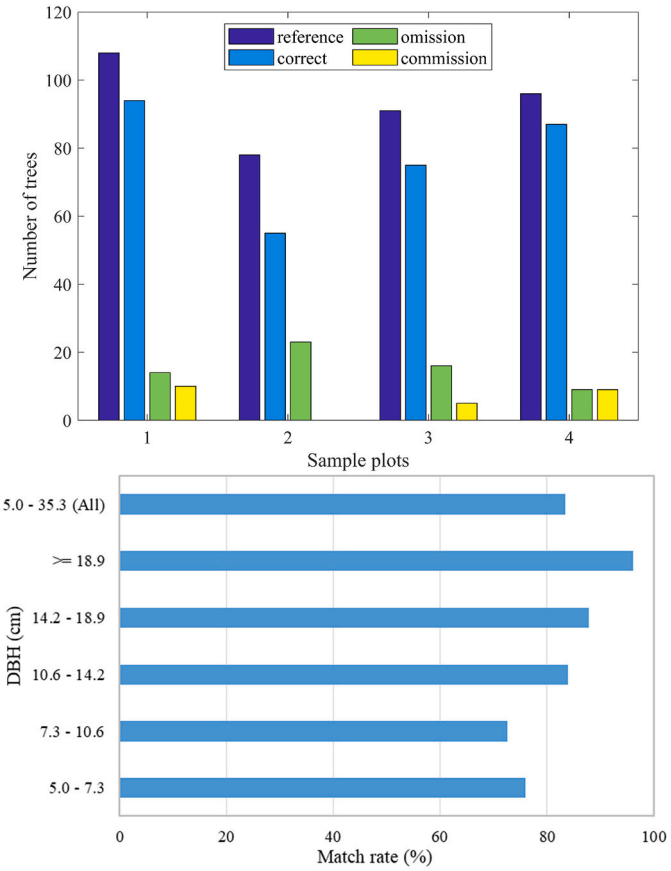

Fig. 3. The number of reference trees, correctly matched LiDAR ITCs, missed trees (omission), and extra ITCs (commission) in four sample plots (upper panel) and the ITC detection rate for different DBH groups (lower panel).

4.2. Individual-tree functional traits

Fig. 4 shows the LiDAR-derived morphological and spectral indices of physiological traits at individual tree level (See Supp Fig. 2 for detailed spatial distribution of each trait). Morphologically, blueish-green areas (e.g., subregion A) near a village at lower altitudes are characterized by high LAI and low canopy height, indicating a disturbed forest area. Green and yellow areas (e.g., subregion B) in the mid-altitude are occupied by forest with lower LAI, taller trees and more complex, layered canopies. Pink areas (e.g., subregion C) close to the ridge represent high LAI values and tall canopies, yet with little layering. Physiologically, in subregion A (blueish-green area) canopies have relatively high nitrogen concentration and SLA, but low carotenoid content. Trees in subregion B show diverse physiological trait patterns, where blue areas indicate canopies with relatively low nitrogen concentration, high SLA and low carotenoid content, while red and yellow areas indicate canopies with relatively high carotenoid content and nitrogen concentration. Trees in subregion C (pink area) have canopies with relatively high SLA and carotenoid content, but low nitrogen concentration. Comparing the spatial patterns of two trait maps, it can also be shown that the physiological traits are linked more strongly to topographic variables such as slope and aspect that may both influence optical properties and species composition.

The LiDAR-derived tree height ($R^2 \geq 0.90$, $P < .001$, Zhao et al., 2018) and LAI values ($R^2 = 0.81$, $P < .001$, Supp Fig. 3) were closely correlated with individual-tree field measurements. Due to the complexity of the within-canopy structure, FHD, describing the foliage arrangement in different vertical strata, could not be validated directly

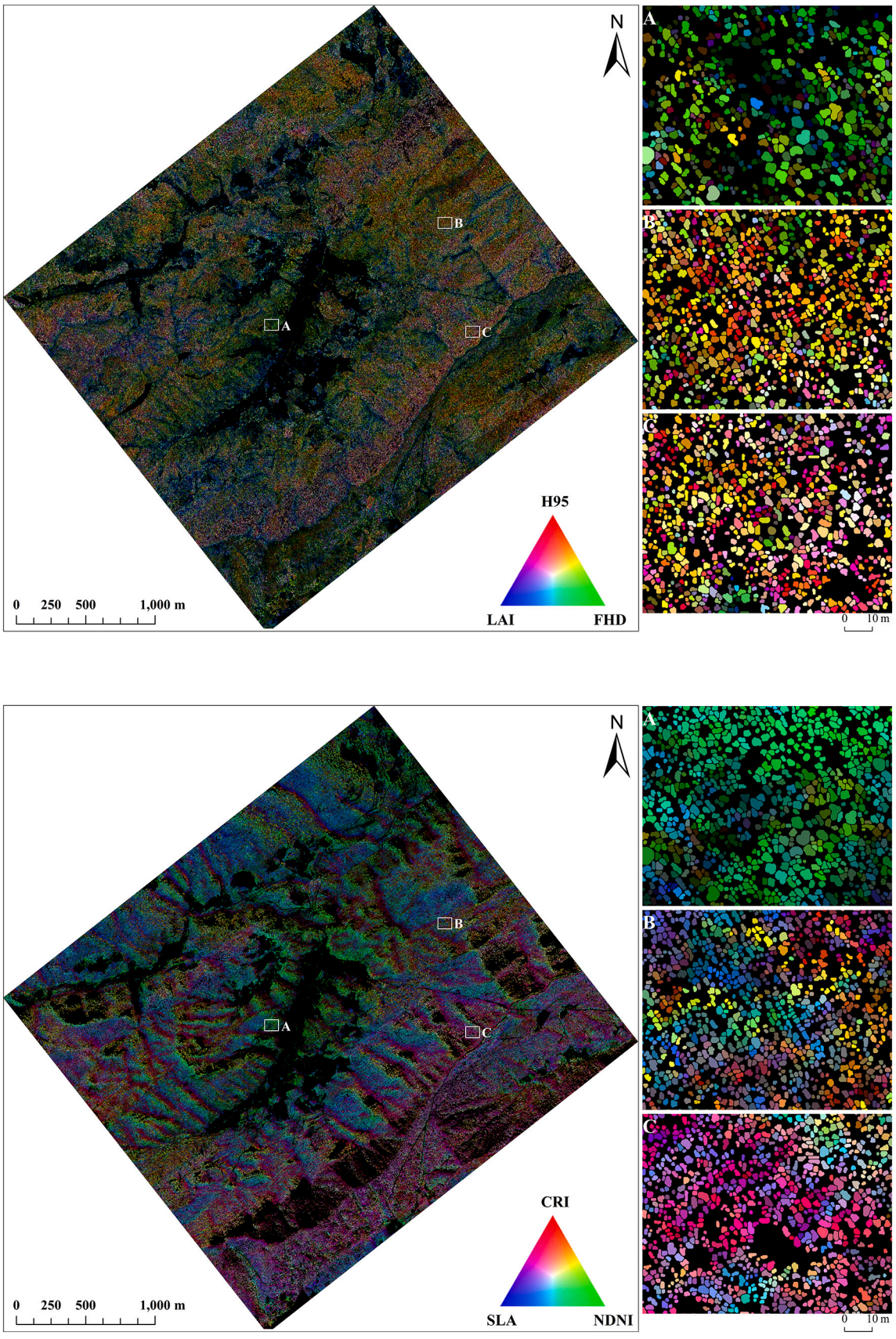

Fig. 4. Spatial patterns of individual-tree morphological and physiological traits in the Longmenhe region. RGB color composites are represented as ternary diagrams of morphological traits (upper panel, 95th quantile height (H_{95}, red), foliage height diversity (FHD, green) and leaf area index (LAI, blue)) and physiological traits (lower panel, carotenoids (CRI, red), nitrogen (NDNI, green) and specific leaf area (SLA, blue)). (For interpretation of the references to colour in this figure legend, the reader is referred to the web version of this article.)

with field measurements. Correlations between the canopy reflectance-based physiological traits and field-sampled individual-tree leaf traits were expectedly less strong than those for the morphological traits, but still very highly significant ($R^2 = 0.60$ for carotenoids, $R^2 = 0.51$ for SLA and $R^2 = 0.34$ for nitrogen, with $n = 31$ and $P < .001$ for all three traits, Supp Fig. 4).

The ranges of the estimated individual tree functional traits in the Longmenhe region are shown in Table 1, where the sample size of trees for morphological trait estimates was 1,145,690 (after masking very dense trees for which we could not retrieve LAI because of no ground echoes) and the sample size of trees for physiological trait estimates was 1,026,737 (after masking trees located in shaded areas) from a total of 1,253,809 detected canopy trees. The normalized H_{95}, LAI and FHD of individual trees have means and standard deviations of 0.38 ± 0.18, 0.38 ± 0.21 and 0.49 ± 0.22, respectively. And the normalized CRI, SLA and NDNI of individual trees have means and standard deviations of 0.55 ± 0.19, 0.51 ± 0.22 and 0.46 ± 0.16, respectively (Supp Fig. 5).

Trait correlation assessment (n = 941,650) showed that LiDAR-derived H_{95} and FHD of individual trees were positively correlated (r = 0.44), while CRI and SLA were negatively correlated (r = −0.29). Correlations between morphological and physiological traits were very weak, but due to the high number of measurements still highly significant (up to $r = 0.11$ between H_{95} and CRI but $r < 0.03$ for all other pairs) (Fig. 5; Supp Fig. 6 a–f).

4.3. Functional diversity

Maps of FRic, FDiv and FEve for morphological and physiological traits for 30 × 30-m resolution are shown in Fig. 6. The highest morphological FRic (Morph.FRic) and morphological FEve (Morph.FEve) occur at medium elevations (1404–1487 m), which is consistent with previous forest community survey studies (Shen et al., 2004; Zhao et al., 2005). High physiological FRic (Phys.FRic) and physiological FEve (Phys.FEve) can be observed at medium and high elevations. Morphological FDiv (Morph.FDiv) has a similar distribution in different elevational zones, but physiological FDiv (Phys.FDiv) shows an obvious elevational pattern (Supp Fig. 7).

We explored the relationship between FRic and tree density (i.e. tree number) for 30 × 30 m grid cells, an area which we considered a relevant ecosystem scale in these forests (Liu et al., 2018). The results showed generally positive relationships between FRic and tree density for both Morph.FRic and Phys.FRic, but the Phys.FRic decreased at very high tree densities (Fig. 7).

4.4. Scaling

The FRic–area curves showed that the ITC-based FRic increased with area (see Supp Fig. 8 for the spatial patterns of FRic at different neighborhood scales) and the observed FRic was relatively lower than the simulated FRic of the null model (Fig. 8). These results indicated the prevalence of local trait convergence in our study area. Fitting power-law and logarithmic functions to the FRic-area relationships, we found the power-law exponents were 0.23 and 0.37 for Morph.FRic and Phys.FRic, while the FRic–log(area) curves were almost linear. Therefore, a logarithmic function fitted the FRic–area relationships better ($R^2 = 0.99$ and 0.98) than the power-law function ($R^2 = 0.85$ and 0.91, Fig. 8). For FRic–tree number relationships, the logarithmic function also fitted the mean observed Morph.FRic and Phys.FRic better ($R^2 = 0.99$ and 0.95) than the power-law function ($R^2 = 0.80$ and 0.88, Supp Fig. 9).

Table 1
Minimum, maximum and mean (SD) values of functional traits of individual trees derived from LiDAR and imaging spectroscopy in the Longmenhe region.

Trait (units)	Min	Max	mean ± SD
H_{95} (m)	5.198	29.060	14.160 ± 4.330
LAI	1.236	6.291	3.131 ± 1.064
FHD	0.188	1.523	0.846 ± 0.298
CRI	3.836	11.922	8.253 ± 1.545
SLA	2.406	4.997	3.735 ± 0.574
NDNI	0.206	0.346	0.271 ± 0.022

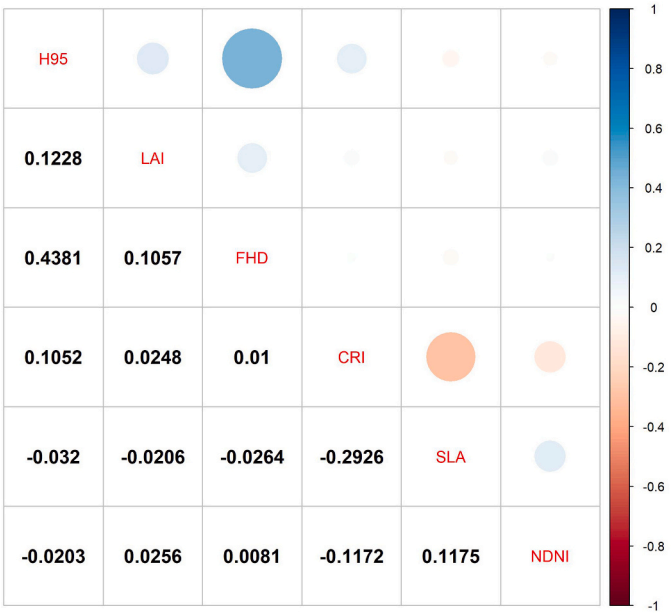

Fig. 5. Pearson correlation matrix of individual-tree functional traits derived by LiDAR and imaging spectroscopy data. Size and shade of each circle represent the strength of the relationship with color indicating significantly positive (blue) or negative (red) correlations. (For interpretation of the references to colour in this figure legend, the reader is referred to the web version of this article.)

5. Discussion

5.1. Individual tree-based trait measurements

Our findings demonstrate the ability of integrating airborne LiDAR and imaging spectroscopy data to estimate individual-tree morphological and physiological traits in a spatially explicit and consistent way at large scales. Compared with mapping functional traits and FD based on pixels or plots representing vegetation samples of potentially mixed species (Durán et al., 2019; Ma et al., 2019; Schneider et al., 2017), our individual tree-based method can directly account for variation between individuals and allows us to combine both within- and between-species FD. However, assigning individuals to species using few remotely-sensed functional traits is challenging, especially for species-diverse forests with functionally similar species. Even by combining both morphological and physiological traits, only slightly more than half of all individuals could be correctly assigned to species, but more than 80% could be correctly assigned to tree functional or taxonomic groups (Text S1; Supp Fig. 10). The groups can be any clustering of individuals for which classification information is available, for example, groups divided according to life forms (deciduous trees vs. evergreen trees vs. shrubs), plant strategies (C, S and R), taxonomic information (conifers vs. angiosperms) or environmental gradients (Durán et al., 2019; Kattenborn et al., 2017; Li et al., 2017; Milani et al., 2019). Furthermore, individual-tree trait measures also allow us to assess plant strategy spectra such as leaf-economics spectra (Asner et al., 2016; Wright et al., 2004) from remotely-sensed large-scale data.

Individual tree-based trait and FD measurements offer ecologically relevant advantages over pixel- or plot-based measurements. For example, the ITC-based approach allows us to explore FRic–tree density relationships in real forests with spatially explicit data, while these can

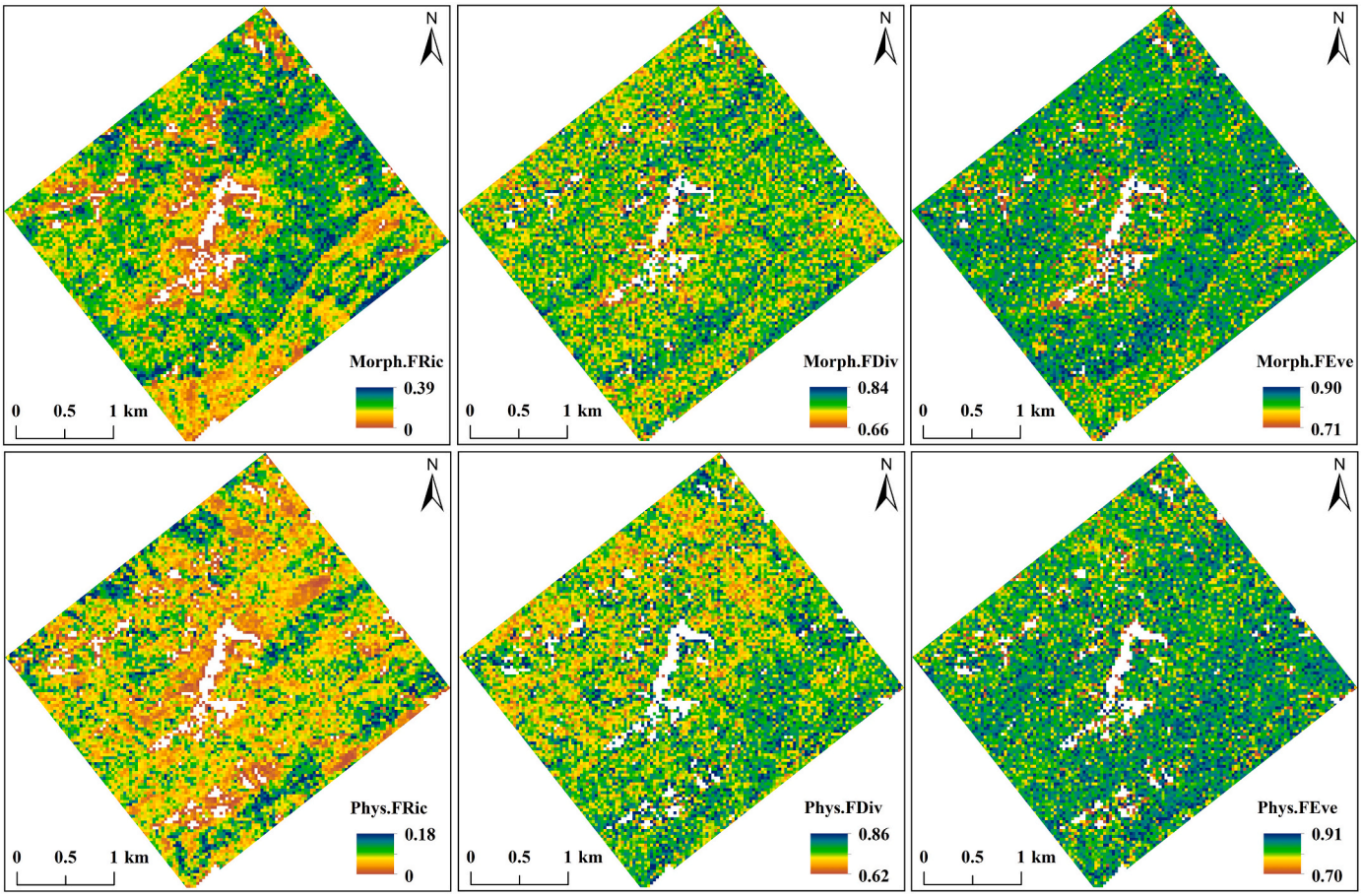

Fig. 6. Spatial patterns of ITC-based morphological (upper panel) and physiological (lower panel) richness (left), divergence (middle) and evenness (right).

not be assessed with pixel- or plot-based approaches, because they do not allow counting individuals or covering large areas. Besides, partitioning trait variation among individuals into taxonomic and potentially genetic variation, environmental variation and their interaction is only possible if traits are measured at individual level. Being able to predict FD using traits that are specific properties of individual trees (e.g., crown size, tree height), the FD assessments could be expanded to include more dimensions representing different facets of plants and links to ecosystem functioning. In addition, the individual-level data do not contain variable biases due to subjective interpretation or different measurement techniques and might improve individual-based ecological models (Fisher et al., 2018). Furthermore, our approach could be useful to interpret within-pixel or within-footprint information of spaceborne imaging spectrometers such as Gaofen-5 (Liu et al., 2019) and NASA's Surface Biology and Geology (SBG, Schneider et al., 2019) or spaceborne LiDAR (e.g., GEDI, Schneider et al., 2020). When using such coarser spatial resolution instruments, it might help to better understand the scaling from individual trees to whole forest canopies and from individual-tree, single-species measurements to individual-pixel, mixed-species measurements from spaceborne sensors. Further comparison of the ITC- vs. pixel-based approach will be needed to fully understand the linkages and differences of individual tree to canopy traits. It can also help to quantify how much of the initial diversity of functional traits can be observed at different pixel sizes, which would be a crucial step for upscaling forest FD effectively (Gonzalez et al., 2020).

The individual tree crown (ITC) detection was the basis to estimate individual-tree functional traits from remote sensing. Our comparisons with field observations indicated that the LiDAR data allowed ITC detection with good accuracy. We could correctly identify more than 80% of ITCs for coniferous forest and more than 70% for broad-leaved forest. Indeed, good accuracy of detecting ITCs with LiDAR was also reported for boreal and temperate forests (Kaartinen et al., 2012; Kwak et al., 2007; Wang et al., 2016a) and will likely further improve in the future. Besides, Bohlman (2015) suggested that diversity measured by remote-sensing platforms that detect primarily the upper canopy layer, would match up well with diversity estimates from forest inventories of trees ≥10 cm DBH in tropical forest. Our assessment of ITC detection rate also showed confidence in detecting larger canopy trees (Fig. 3). In addition, compared with forest inventories with a limited number of sampling plots and a bias towards large-tree selection, as well as limited access to inaccessible regions, our ITC-based method detected 70%–90% of all canopy trees (≥5-cm DBH) and has the advantage of covering all environmental gradients over large areas. Although uncertainty propagation and associated bias in trait estimates can still exist due to under- or over-segmentation, the undetected trees (e.g., sub-canopy tree individuals or even tree saplings) tend to be smaller ones with presumably less influence on ecosystem-level functions (Jeronimo et al., 2018; Moore et al., 2007). More critical errors would result from additional trees being detected by LiDAR, which do not exist on the ground (commission errors), because these would be like pixel-based measures including (parts of) one or several trees possibly belonging to different species. Fortunately, such commission errors were less than 10% in our four calibration plots. The accuracy of ITC detection and matching with imaging spectroscopy data may suffer from overlapping crowns, varying LiDAR point densities or vertical resolution, crown segmentation algorithms, geometric co-alignment issues and the resolution of the imaging spectroscopy data (Dalponte and Coomes, 2016; Ørka et al., 2009, 2010). It is also important to note that our ITC detection is limited to the canopy crowns visible to both, the airborne LiDAR and imaging spectrometer, and therefore does not include understory trees. However,

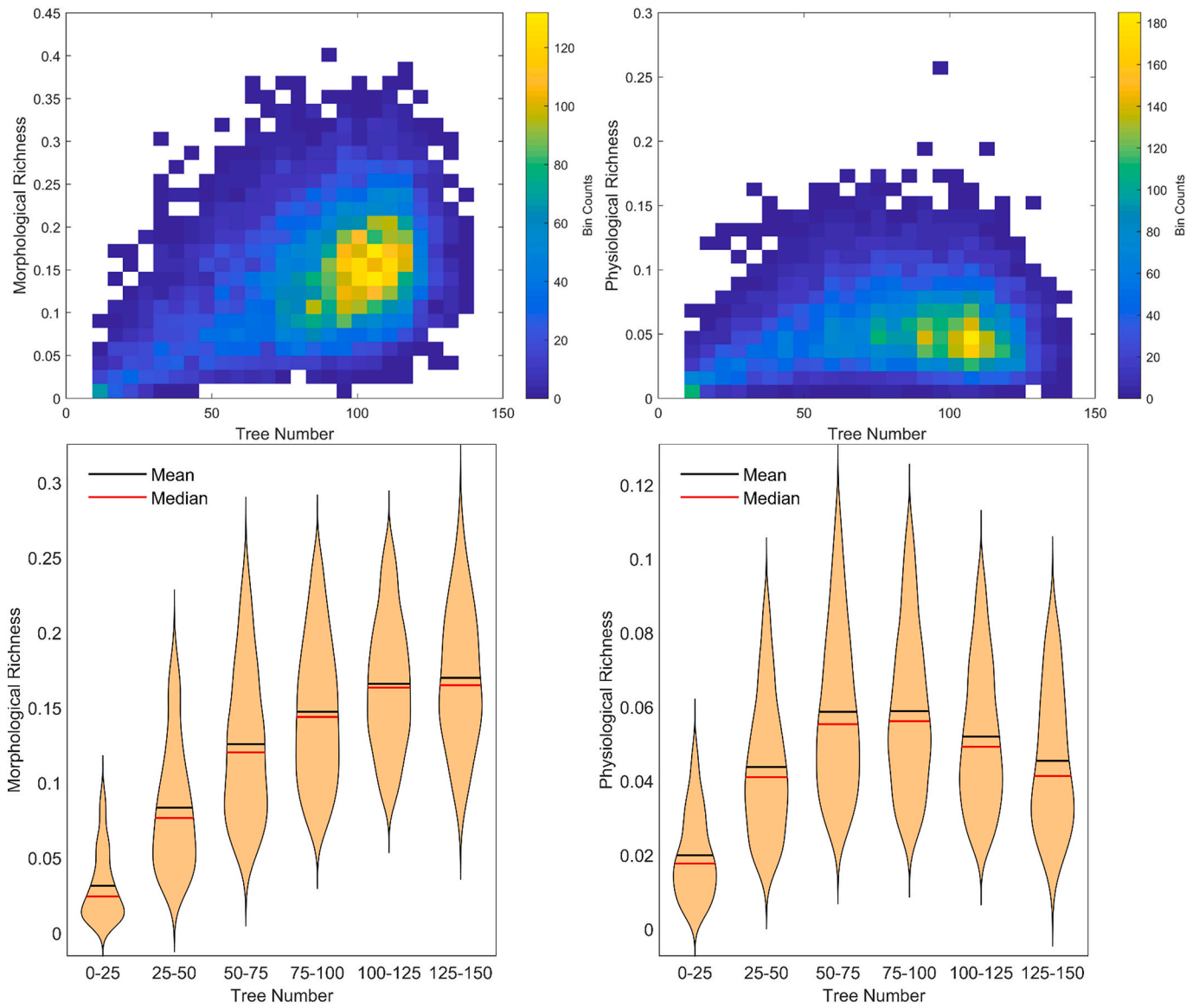

Fig. 7. Relationship between functional richness and tree density per 30 × 30 m plots for morphological richness (left) and physiological richness (right). The upper panels are the binned scatterplots of functional richness and tree density. The lower panels are the violin plots of functional richness (between the 5th and 95th percentile) in different tree density groups.

ecosystem functions are strongly affected by canopy trees (Ali et al., 2019; Liu et al., 2018) and thus omitting understory trees is probably a smaller issue than inaccurate identification of canopy trees. In the future, high-resolution and multitemporal LiDAR data, potentially fused with imaging data, and development of better crown segmentation algorithms may allow us to improve the ITC detection.

5.2. Functional trait selection and retrieval

Our selected morphological traits represent the three primary structural axes — height, openness and complexity of canopy structure — which have been widely used to characterize the canopy structural diversity (Coops et al., 2016; Fahey et al., 2019; Simonson et al., 2012). The selected physiological traits are related to growth/photosynthesis, metabolic cycle, leaf survival/protection and longevity (Díaz et al., 2016; Jetz et al., 2016; Wright et al., 2004). They cover several facets of forest properties linked to ecosystem functioning and are not highly correlated. Further traits with well-known contributions to tree growth, reproduction and survival and thus vegetation dynamics and ecosystem functioning should be included in future assessments, if sensitive indices for such traits can be derived. Such traits include phosphorus, lignin, cellulose, equivalent water thickness of leaves, which are related to growth and defense (survival), canopy volume and position related to competition for light and space, wood density related to persistence and flowering and fruiting phenology and seed mass related to reproduction (Williams et al., 2017; Liu et al., 2016; Westoby, 1998). Additionally, previous studies indicated that the ability to predict community composition could increase with additional traits, but might reach saturation after including a specific number of trait axes (Laughlin, 2014; Schweiger et al., 2020). Therefore, the number and type of traits and methods of extracting meaningful axes to characterize the multivariate trait space, such as principle component analysis, are also important considerations when converting trait measures to FD indices.

The individual tree–trait calibration and validation remains challenging, especially for canopy physiological traits due to variability in canopy reflectance caused by complex canopy structure, signals of non-leaf material in gaps, the atmosphere and changing illumination and viewing geometries (Asner and Martin, 2008; Cavender-Bares et al.,

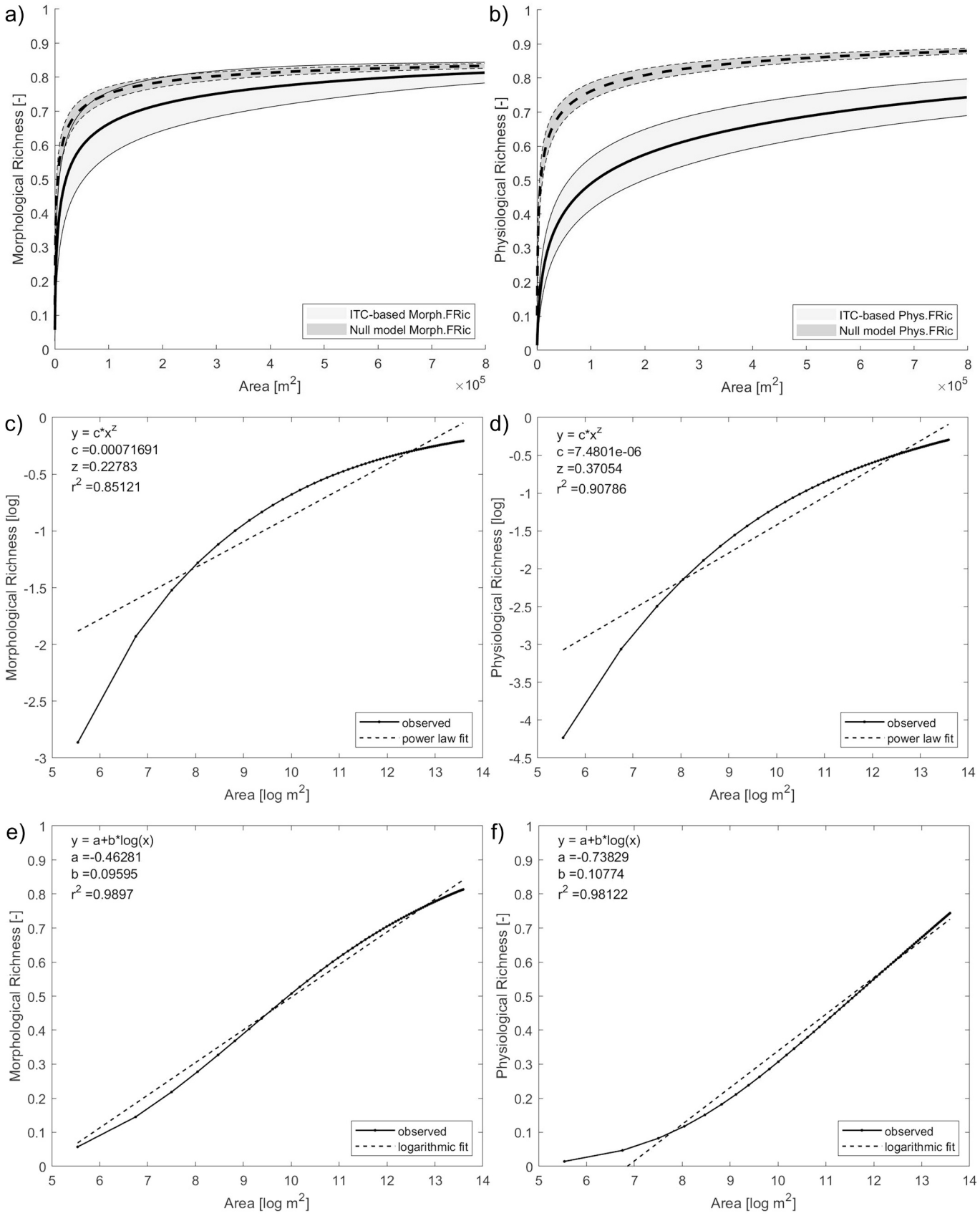

Fig. 8. Morphological (left panels) and physiological (right panels) functional richness–area relationships. Null models correspond to randomly distributed traits (dashed line); remotely-sensed relationships are depicted as solid line; Grey shades indicate the standard deviations of all 3 × 3 m grid cells of forest area (a, b). The log(FRic)–log(area) curves in the middle panels represent the fit of power-law functions (c, d) and the FRic–log(area) curves in the lower panels represent the fit of a logarithmic function (e, f) for morphological and physiological richness.

2017; Ollinger, 2011). Further difficulties are due to temporal mismatches between in-situ and airborne data (Chavana-Bryant et al., 2017), uncertainties introduced by ITC segmentation (Marconi et al., 2019b) and downscaling to leaf traits at leaf level from the ITC measures at canopy level (Gara et al., 2018; Homolová et al., 2013; Malenovský et al., 2019). Accordingly, our LiDAR-derived individual-tree morphological traits correlated better with independent field-based measurements than did our canopy reflectance-based physiological traits with laboratory measurements (Supp Fig. 4). Vegetation index-based physiological trait estimations can be processed faster than radiative transfer model-based retrievals and thus have seen a wider applicability over large areas. Since VIs only make use of a small set of spectral bands, the selection of optimal VIs to indicate the relevant physiological traits should be carefully evaluated. To improve the effectiveness and accuracy of canopy-level physiological trait estimation from imaging spectroscopy data, other methods such as multi-method ensemble and the Gaussian process-based emulators of radiative transfer models have been used (Feilhauer et al., 2015; Gómez-Dans et al., 2016; Verrelst et al., 2015, 2019). If sufficient training data are available, PLSR or machine learning regression models can be effective alternatives making use of the full reflectance spectrum. Moreover, recent studies have explored the potential of using airborne imaging spectroscopy and LiDAR data or hyperspectral LiDAR technology to map 3D profiles of foliar traits (Chlus et al., 2020; Nevalainen et al., 2014). Combining LiDAR and imaging spectroscopy data to characterize plant functional traits and diversity enables a broader view of plant form and function, integrating three-dimensional tree architecture with leaf biophysical and biochemical properties.

Furthermore, it should be noted that the optical-based physiological trait retrievals might be sensitive to illumination conditions. In this study, we used a CRI threshold to mask shadow pixels, which removed the overestimation of carotenoids and underestimation of SLA in the shade. The derived physiological traits then can represent the ecological pattern of traits between sunny and shaded slopes. For example, Han et al. (2005) found that leaf N were significantly higher in deciduous than in evergreen species. Tian et al. (2002) showed that in the Longmenhe region, deciduous tree species grow well on ridges, while evergreen tree species mostly occur in shaded areas or humid valleys. Consistently, our derived nitrogen concentration also showed higher values on ridges and lower values in valleys and shaded slopes.

Assessing correlations between the estimated traits showed a positive correlation between H_{95} and FHD and a negative correlation between carotenoids and SLA, consistent with previous studies (Martin et al., 2007). However, the trait correlations at individual tree level in our study were not as strong as those in other works reporting species- or plot-level correlations (Osnas et al., 2018). It is typical that zooming into broad-scale macro-ecological correlations reveals many more facets of trait coordination (Li et al., 2017), which is brushed over when much larger scales are considered (Wright et al., 2004). Thus, trade-offs are often stronger at the genetic or phylogenetic level or in between-site comparisons than within species and sites (Messier et al., 2017; Umaña and Swenson, 2019).

5.3. Functional diversity and tree density

We explored the FRic–tree density relationship for the 30 × 30 m ecosystem scale and found generally positive relationships between morphological and physiological FRic and tree density. Similar positive relationships were also found in forest inventories relating tree species richness to stand density, indicating a higher carrying capacity in mixed forests due to the complementarity of resource uses and reduced mortality (Baruffol et al., 2013; Pretzsch and Biber, 2016). A decrease in FRic at very high tree densities was also observed in previous studies showing that the species richness of vascular plants decreased with stand density at intermediate or high forest densities (Hedwall et al., 2019). One explanation is that these areas were dominated by many young trees or forest patches planted with the same species. More research is needed to reveal cause and effect relationships between FD and tree density (Condés and del Río, 2015; Pretzsch et al., 2015), which may change with scale due to the scale-dependency of FD (see below) but scale-invariance of density. Forest diversity might also affect tree density in natural forests through its influence on resilience to disturbances. For example, individual trees and forest populations may be particularly vulnerable to extreme climatic events or insect attacks by reduced diversity and limited stand structural complexity (Návar, 2019). Therefore, it is important to take the FD and tree density relationship into account when guiding forest management and conservation, and analyzing the relationship between diversity and ecosystem functioning (Baruffol et al., 2013; Forrester and Bauhus, 2016; Ouyang et al., 2019).

5.4. Scale dependency of functional diversity

The species richness–area relationship, a well-established empirical power-law relationship in ecology, has been applied widely in biodiversity conservation (Gerstner et al., 2014) and one might expect a similar relationship with FRic (Karadimou et al., 2016; Schneider et al., 2017). In our case the exponent or slope of the log-log regression was 0.228 for morphological FRic, which is similar to the slope for species richness–area relationship across large ranges, i.e. 0.212–0.267 in Gerstner et al. (2014), but much larger than for species–area relationships across similarly narrow ranges as tested for our FD–area relationships, e.g. 0.062–0.106 in Peintinger et al. (2003). The slope for physiological FRic–area relationship (0.371) was even higher, suggesting that the turnover of functional β-diversity may be higher than the turnover of species. We speculate that underdispersion of functional traits due to strong environmental filtering at small scales combined with environmental heterogeneity creates different filtering at larger scales. However, these results may in part also be affected by the fact that the shape of our FD–area relationships were in fact better matched by a simple logarithmic relationship, where FD was modelled as a linear function of log(area), a result similar to the pixel-based FD–area relationship analyzed in Schneider et al. (2017). The logarithmic relationship indicates that the FD–area curve flattens out more strongly at large scales than is generally the case for species richness, indicating that the additional species at larger scales are likely functionally redundant with other species already present.

By comparing FRic–area relationships of remotely-sensed traits with spatially randomly distributed traits (null model), we found trait convergence, i.e. functional underdispersion, to be predominant at local scales in our study area. As mentioned above, this could be due to environmental filtering at small scale combined with environmental heterogeneity at larger scales, heterogeneity in forest management strategies or, less likely, due to dispersal being strongly local (Botta-Dukát and Czúcz, 2016).

Besides, we can also regard the tree number as a scale and calculate diversity measures per number of individual trees in a sample, not only per area. We found that the FRic also linearly increases with the logarithm of tree number, which can be used for FRic corrections of different numbers of trees per area, i.e. different tree densities, which is important to study density-dependent effects (Antonovics and Levin, 1980; Harper, 1977; Wills et al., 1997) and the mechanisms that link biodiversity with ecosystem functions (Baruffol et al., 2013; Williams et al., 2017).

6. Conclusions

In this study, we developed a spatially complete individual tree-based method to map FD using LiDAR-derived morphological traits and hyperspectral reflectance-based physiological traits in a subtropical forest in China. In contrast to the FD estimation based on pixels or plots, the method described here avoids mixing of different species within the smallest unit of observation and thus allows us to move from canopy-

level to individual-level trait mapping. Being able to predict FD using individual-tree functional traits not only explains trait variation along environmental gradients, but also offers opportunities to explore trade-offs between traits and FD–tree density relationships at within- and between-ecosystem scales. These relationships are essential to better understand the mechanisms that link biodiversity with ecosystem functions. Our individual tree-based method also opens up a large number of additional directions for analyses, for example those used in community ecology using field-based trait measurements. If ITCs could be assigned to life forms, functional types (for grassland see Kattenborn et al., 2017; Schmidtlein et al., 2012) and eventually species by improving classification of trees, many ecological analyses that are currently restricted by small sample sizes of field-measured trees can then be applied on spatially complete sets of almost all trees present in an area.

As contemporary remote sensing data (LiDAR, imaging spectroscopy and high-resolution images) as well as computational power are becoming more accessible, it becomes increasingly feasible to use ITC approaches for identifying different species, tree size (age) and tree phenological stages, as well as environmental conditions and management practices, allowing us to better understand inter- and intra-specific variation and predict ecosystem functions (e.g., productivity, evapotranspiration and ecosystem resilience) in the context of global change drivers. Further scaling studies will reveal to what level FD can be measured from different remote sensing data, providing the potential to bridge the scale gap between local field plots, regional airborne and global spaceborne observations. Such data will also be able to refine next-generation global vegetation models. Considering that different ecosystems may display different scale dependency of FD (Schneider et al., 2017; Durán et al., 2019; Malenovský et al., 2019), we suggest to develop methodologies based on multi-source data in different biomes to comprehensively evaluate the scalability of our approach and better understand the potentials and challenges of improving remote sensing of traits and FD at different scales.

CRediT author statement

Z. Zheng: conceptualization, data curation, formal analysis, methodology, software, validation, visualization, writing - original draft.

Y. Zeng: conceptualization, supervision, resources, writing - original draft, writing - review & editing.

F.D. Schneider: methodology, software, writing - review & editing.

Y. Zhao: investigation, data curation, writing - review & editing.

D. Zhao: investigation, software, writing - review & editing.

B. Schmid: conceptualization, methodology, writing - review & editing.

M.E. Schaepman: conceptualization, supervision, writing - review & editing.

F. Morsdorf: conceptualization, supervision, methodology, writing - review & editing.

Declaration of Competing Interest

The authors declare that they have no known competing financial interest or personal relationships that could have appeared to influence the work reported in this paper.

Acknowledgements

This study was supported by the National Key Research and Development Program of China (2016YFC0500201) and National Natural Science Foundation of China (No. 42071344 and 41771464). The contributions of ZZ, FM, BS and MES were supported by the University of Zurich Research Priority Program on Global Change and Biodiversity (URPP GCB). The research carried out at the Jet Propulsion Laboratory, California Institute of Technology, was under a contract with the National Aeronautics and Space Administration (80NM0018D0004). U. S. Government sponsorship is acknowledged. The authors thank Zongqiang Xie, Wenting Xu, and Changming Zhao from the Shengnongjia Biodiversity Research Station of the Chinese Academy of Science for their support with fieldwork. We also thank Xinfeng Zhao, Liang Zhu, Wenxue Dong, Zilong Yang, Zhugeng Duan, Wenwen Gao and Hong Chi for their assistance with the field sample collection. We appreciate the anonymous reviewers for constructive comments on our manuscript and thank to Victoria Scholl for discussions on ITC detection. The acquisition and preprocessing of airborne LiDAR and imaging spectroscopy data were supported by the Shanghai Hangyao Information Technology Cooperation. ZZ acknowledges financial support from the China Scholarship Council (Grant No. 201704910941).

Appendix A. Supplementary data

Supplementary data to this article can be found online at https://doi.org/10.1016/j.rse.2020.112170.

References

Ahmed, D.A., van Bodegom, P.M., Tukker, A., 2019. Evaluation and selection of functional diversity metrics with recommendations for their use in life cycle assessments. Int. J. Life Cycle Assess. 24 (3), 485–500.

Ali, A., Lin, S.L., He, J.K., Kong, F.M., Yu, J.H., Jiang, H.S., 2019. Big-sized trees overrule remaining trees' attributes and species richness as determinants of aboveground biomass in tropical forests. Glob. Chang. Biol. 25, 2810–2824.

Ammer, C., Fichtner, A., Fischer, A., Gossner, M.M., Meyer, P., Seidl, R., 2018. Key ecological research questions for Central European forests. Basic Appl. Ecol. 32, 3–25.

Antonovics, J., Levin, D.A., 1980. The ecology and genetics of density-dependent regulation in plants. Annu. Rev. Ecol. Syst. 11 (1), 411–452.

Asner, G.P., Martin, R.E., 2008. Spectral and chemical analysis of tropical forests: scaling from leaf to canopy levels. Remote Sens. Environ. 112 (10), 3958–3970.

Asner, G.P., Martin, R.E., 2009. Airborne spectranomics: mapping canopy chemical and taxonomic diversity in tropical forests. Front. Ecol. Environ. 7 (5), 269–276.

Asner, G.P., Knapp, D.E., Anderson, C.B., Martin, R.E., Vaughn, N., 2016. Large-scale climatic and geophysical controls on the leaf economics spectrum. Proc. Natl. Acad. Sci. 113 (28), E4043–E4051.

Asner, G.P., Martin, R.E., 2016. Spectranomics: emerging science and conservation opportunities at the interface of biodiversity and remote sensing. Glob. Ecol. Conserv. 8, 212–219.

Asner, G.P., Martin, R.E., Anderson, C.B., Knapp, D.E., 2015. Quantifying forest canopy traits: imaging spectroscopy versus field survey. Remote Sens. Environ. 158, 15–27.

Asner, G.P., Martin, R.E., Knapp, D.E., Tupayachi, R., Anderson, C.B., Sinca, F., et al., 2017. Airborne laser-guided imaging spectroscopy to map forest trait diversity and guide conservation. Science 355 (6323), 385–389.

Baruffol, M., Schmid, B., Bruelheide, H., Chi, X., Hector, A., Ma, K., et al., 2013. Biodiversity promotes tree growth during succession in subtropical forest. PLoS One 8 (11), e81246.

Bohlman, S.A., 2015. Species diversity of canopy versus understory trees in a neotropical forest: Implications for forest structure, function and monitoring. Ecosystems 18, 658–670.

Bongers, F., Schmid, B., Sun, Z., Li, Y., Härdtle, W., von Oheimb, G., et al., 2020. Growth–trait relationships in subtropical forest are stronger at higher diversity. J. Ecol. 108, 256–266.

Botta-Dukát, Z., Czúcz, B., 2016. Testing the ability of functional diversity indices to detect trait convergence and divergence using individual-based simulation. Methods Ecol. Evol. 7, 114–126.

Cadotte, M.W., Carscadden, K., Mirotchnick, N., 2011. Beyond species: functional diversity and the maintenance of ecological processes and services. J. Appl. Ecol. 48 (5), 1079–1087.

Carmona, C.P., de Bello, F., Mason, N.W.H., Lepš, J., 2016. Traits without borders: integrating functional diversity across scales. Trends Ecol. Evol. 31 (5), 382–394.

Casas, A., Riaño, D., Ustin, S.L., Dennison, P., Salas, J., 2014. Estimation of water-related biochemical and biophysical vegetation properties using multitemporal airborne hyperspectral data and its comparison to MODIS spectral response. Remote Sens. Environ. 148, 28–41.

Cavender-Bares, J., Gamon, J.A., Hobbie, S.E., Madritch, M.D., Meireles, J.E., Schweiger, A.K., et al., 2017. Harnessing plant spectra to integrate the biodiversity sciences across biological and spatial scales. Am. J. Bot. 104, 966–969.

Chadwick, K.D., Asner, G.P., 2016. Organismic-scale remote sensing of canopy foliar traits in lowland tropical forests. Remote Sens. 8 (2), 87.

Chavana-Bryant, C., Malhi, Y., Wu, J., Asner, G.P., Anastasiou, A., Enquist, B.J., et al., 2017. Leaf aging of Amazonian canopy trees as revealed by spectral and physiochemical measurements. New Phytol. 214, 1049–1063.

Chen, Q., Baldocchi, D., Gong, P., Kelly, M., 2006. Isolating individual trees in a savanna woodland using small footprint Lidar data. Photogramm. Eng. Remote. Sens. 72, 923–932.

Chen, J.M., Rich, P.M., Gower, S.T., Norman, J.M., Plummer, S., 1997. Leaf area index of boreal forests: theory, techniques, and measurements. J. Geophys. Res. 102 (D24), 29429–29443.
Chlus, A., Kruger, E.L., Townsend, P.A., 2020. Mapping three-dimensional variation in leaf mass per area with imaging spectroscopy and lidar in a temperate broadleaf forest. Remote Sens. Environ. 250, 112043.
Clark, J.S., Bell, D.M., Hersh, M.H., Kwit, M.C., Moran, E., Salk, C., et al., 2011. Individual-scale variation, species-scale differences: inference needed to understand diversity. Ecol. Lett. 14, 1273–1287.
Clawges, R., Vierling, K., Vierling, L., Rowell, E., 2008. The use of airborne lidar to assess avian species diversity, density, and occurrence in a pine/aspen forest. Remote Sens. Environ. 112 (5), 2064–2073.
Condés, S., del Río, M., 2015. Climate modifies tree interactions in terms of basal area growth and mortality in monospecific and mixed *Fagus sylvatica* and *Pinus sylvestris* forests. Eur. J. For. Res. 134 (6), 1095–1108.
Coops, N.C., Tompaski, P., Nijland, W., Rickbeil, G.J.M., Nielsen, S.E., Bater, C.W., et al., 2016. A forest structure habitat index based on airborne laser scanning data. Ecol. Indic. 67, 346–357.
Cornwell, W.K., Schwilk, D.W., Ackerly, D.D., 2006. A trait-based test for habitat filtering: convex hull volume. Ecology 87, 1465–1471.
Dalponte, M., Coomes, D.A., 2016. Tree-centric mapping of forest carbon density from airborne laser scanning and hyperspectral data. Methods Ecol. Evol. 7 (10), 1236–1245.
Díaz, S., Cabido, M., 2001. Vive la différence: plant functional diversity matters to ecosystem processes. Trends Ecol. Evol. 16, 646–655.
Díaz, S., Fargione, J., Chapin III, F.S., Tilman, D., 2006. Biodiversity loss threatens human well-being. PLoS Biol. 4, e277.
Díaz, S., Kattge, J., Cornelissen, J.H.C., Wright, I.J., Lavorel, S., Dray, S., et al., 2016. The global spectrum of plant form and function. Nature 529, 167–171.
Duffy, J.E., Godwin, C.M., Cardinale, B.J., 2017. Biodiversity effects in the wild are common and as strong as key drivers of productivity. Nature 549, 261–264.
Duncanson, L., Dubayah, R., 2018. Monitoring individual tree-based change with airborne lidar. Ecol. Evol. 8 (10), 5079–5089.
Durán, S.M., Martin, R.E., Díaz, S., Maitner, B.S., Malhi, Y., Salinas, N., et al., 2019. Informing trait-based ecology by assessing remotely sensed functional diversity across a broad tropical temperature gradient. Sci. Adv. 5 (12), eaaw8114.
Ewald, M., Aerts, R., Lenoir, J., Fassnacht, F.E., Nicolas, M., Skowronek, S., et al., 2018a. LiDAR derived forest structure data improves predictions of canopy N and P concentrations from imaging spectroscopy. Remote Sens. Environ. 211, 13–25.
Ewald, M., Skowronek, S., Aerts, R., Dolos, K., Lenoir, J., Nicolas, M., et al., 2018b. Analyzing remotely sensed structural and chemical canopy traits of a forest invaded by *Prunus serotina* over multiple spatial scales. Biol. Invasions 20 (8), 2257–2271.
Fahey, R.T., Atkins, J.W., Gough, C.M., Hardiman, B.S., Nave, L.E., Tallant, J.M., et al., 2019. Defining a spectrum of integrative trait-based vegetation canopy structural types. Ecol. Lett. 22, 2049–2059.
Fang, J., Shen, Z., Tang, Z., Wang, X., Wang, Z., Feng, J., et al., 2012. Forest community survey and the structural characteristics of forests in China. Ecography 35 (12), 1059–1071.
Feilhauer, H., Asner, G.P., Martin, R.E., 2015. Multi-method ensemble selection of spectral bands related to leaf biochemistry. Remote Sens. Environ. 164, 57–65.
Féret, J.B., Francois, C., Gitelson, A., Asner, G.P., Barry, K.M., Panigada, C., et al., 2011. Optimizing spectral indices and chemometric analysis of leaf chemical properties using radiative transfer modeling. Remote Sens. Environ. 115 (10), 2742–2750.
Féret, J.B., le Maire, G., Jay, S., Berveiller, D., Bendoula, R., Hmimina, G., et al., 2019. Estimating leaf mass per area and equivalent water thickness based on leaf optical properties: potential and limitations of physical modeling and machine learning. Remote Sens. Environ. 231, 110959.
Ferreira, M.P., Féret, J.B., Grau, E., Gastellu-Etchegorry, J.P., Shimabukuro, Y.E., de Souza Filho, C.R., 2018. Retrieving structural and chemical properties of individual tree crowns in a highly diverse tropical forest with 3D radiative transfer modeling and imaging spectroscopy. Remote Sens. Environ. 211, 276–291.
Fisher, R.A., Koven, C.D., Anderegg, W.R.L., Christoffersen, B.O., Dietze, M.C., Farrior, C. E., et al., 2018. Vegetation demographics in earth system models: a review of progress and priorities. Glob. Chang. Biol. 24 (1), 35–54.
Flores-Moreno, H., Fazayeli, F., Banerjee, A., Datta, A., Kattge, J., Butler, E.E., et al., 2019. Robustness of trait connections across environmental gradients and growth forms. Glob. Ecol. Biogeogr. 28, 1806–1826.
Forrester, D.I., Bauhus, J., 2016. A review of processes behind diversity—productivity relationships in forests. Curr. Forestry Rep. 2, 45–61.
Fyllas, N.M., Bentley, L.P., Shenkin, A., Asner, G.P., Atkin, O.K., Díaz, S., et al., 2017. Solar radiation and functional traits explain the decline of forest primary productivity along a tropical elevation gradient. Ecol. Lett. 20, 730–740.
Gamon, J.A., Somers, B., Malenovský, Z., Middleton, E.M., Rascher, U., Schaepman, M. E., 2019. Assessing vegetation function with imaging spectroscopy. Surv. Geophys. 40, 489–513.
Gara, T.W., Skidmore, A.K., Darvishzadeh, R., Wang, T., 2018. Leaf to canopy upscaling approach affects the estimation of canopy traits. GISci. Remote Sens. 56 (4), 554–575.
Garnier, E., Navas, M.-L., 2012. A trait-based approach to comparative functional plant ecology: concepts, methods and applications for agroecology. A review. Agron. Sustain. Dev. 32, 365–399.
Garrigues, S., Lacaze, R., Baret, F., Morisette, J.T., Weiss, M., Nickeson, J.E., et al., 2008. Validation and intercomparison of global leaf area index products derived from remote sensing data. J. Geophys. Res. 113, G02028.
Ge, J., Wu, J., Zhu, Z., Zhao, B., 1997. Studies on plant diversity and present situation of conservation in Shennongjia biosphere reserve, Hubei. China. J. Wuhan Bot. Res. 15, 341–352.
Gerstner, K., Dormann, C.F., Václavík, T., Kreft, H., Seppelt, R., 2014. Accounting for geographical variation in species–area relationships improves the prediction of plant species richness at the global scale. J. Biogeogr. 41 (2), 261–273.
Gitelson, A.A., Zur, Y., Chivkunova, O.B., Merzlyak, M.N., 2002. Assessing carotenoid content in plant leaves with reflectance spectroscopy. Photochem. Photobiol. 75 (3), 272–281.
Gómez-Dans, J.L., Lewis, P.E., Disney, M., 2016. Efficient emulation of radiative transfer codes using Gaussian processes and application to land surface parameter inferences. Remote Sens. 8, 119.
Gonzalez, A., Germain, R.M., Srivastava, D.S., Filotas, E., Dee, L.E., Gravel, D., et al., 2020. Scaling-up biodiversity-ecosystem functioning research. Ecol. Lett. 23, 757–776.
Han, W., Fang, J., Guo, D., Zhang, Y., 2005. Leaf nitrogen and phosphorus stoichiometry across 753 terrestrial plant species in China. New Phytol. 168, 377–385.
Harper, J.L., 1977. Population Biology of Plants. Academic Press, London.
Hedwall, P.-O., Holmström, E., Lindbladh, M., Felton, A., 2019. Concealed by darkness: how stand density can override the biodiversity benefits of mixed forests. Ecosphere 10 (8), e02835.
Hill, J., Buddenbaum, H., Townsend, P.A., 2019. Imaging spectroscopy of forest ecosystems: perspectives for the use of space-borne hyperspectral earth observation systems. Surv. Geophys. 40, 553–588.
Homolová, L., Malenovský, Z., Clevers, J.G.P.W., García-Santos, G., Schaepman, M.E., 2013. Review of optical-based remote sensing for plant trait mapping. Ecol. Complex. 15, 1–16.
Hooper, D.U., Chapin III, F.S., Ewel, J.J., Hector, A., Inchausti, P., Lavorel, S., et al., 2005. Effects of biodiversity on ecosystem functioning: a consensus of current knowledge. Ecol. Monogr. 75, 3–35.
Huang, Y., Chen, Y., Castro-Izaguirre, N., Baruffol, M., Brezzi, M., Lang, A., et al., 2018. Impacts of species richness on productivity in a large-scale subtropical forest experiment. Science 362 (6410), 80–83.
Ishii, H.T., Tanabe, S., Hiura, T., 2004. Exploring the relationships among canopy structure, stand productivity, and biodiversity of temperate forest ecosystems. For. Sci. 50 (3), 342–355.
Jeronimo, S.M.A., Kane, V.R., Churchill, D.J., McGaughey, R.J., Franklin, J.F., 2018. Applying LiDAR individual tree detection to management of structurally diverse forest landscapes. J. For. 116, 336–346.
Jetz, W., Cavender-Bares, J., Pavlick, R., Schimel, D., Davis, F., Asner, G., et al., 2016. Monitoring plant functional diversity from space. Nat. Plants 2, 16024.
Jordan, C.F., 1969. Derivation of leaf-area index from quality of light on the forest floor. Ecology 50 (4), 663–666.
Juchheim, J., Ehbrecht, M., Schall, P., Ammer, C., Seidel, D., 2020. Effect of tree species mixing on stand structural complexity. Forestry 93 (1), 75–83.
Kaartinen, H., Hyyppä, J., Yu, X., Vastaranta, M., Hyyppä, H., Kukko, A., et al., 2012. An international comparison of individual tree detection and extraction using airborne laser scanning. Remote Sens. 4 (4), 950–974.
Karadimou, E.K., Kallimanis, A.S., Tsiripidis, I., Dimopoulos, P., 2016. Functional diversity exhibits a diverse relationship with area, even a decreasing one. Sci. Rep. 6, 35420.
Kattenborn, T., Fassnacht, F.E., Pierce, S., Lopatin, J., Grime, J.P., Schmidtlein, S., 2017. Linking plant strategies and plant traits derived by radiative transfer modelling. J. Veg. Sci. 28 (4), 717–727.
Kattge, J., Díaz, S., Lavorel, S., Prentice, I.C., Leadley, P., Bönisch, G., et al., 2011. Try – a global database of plant traits. Glob. Chang. Biol. 17 (9), 2905–2935.
Kattge, J., Bönisch, G., Díaz, S., Lavorel, S., Prentice, I.C., Leadley, P., et al., 2020. TRY plant trait database – enhanced coverage and open access. Glob. Chang. Biol. 26 (1), 119–188.
Koetz, B., Sun, G.Q., Morsdorf, F., Ranson, K.J., Kneubuhler, M., Itten, K., et al., 2007. Fusion of imaging spectrometer and LIDAR data over combined radiative transfer models for forest canopy characterization. Remote Sens. Environ. 106, 449–459.
Korhonen, L., Hadi Packalen, P., Rautiainen, M., 2017. Comparison of Sentinel-2 and Landsat 8 in the estimation of boreal forest canopy cover and leaf area index. Remote Sens. Environ. 195, 259–274.
Kwak, D.-A., Lee, W.-K., Lee, J.-H., Biging, G.S., Gong, P., 2007. Detection of individual trees and estimation of tree height using LiDAR data. J. For. Res. 12, 425–434.
Laliberté, E., Legendre, P., 2010. A distance-based framework for measuring functional diversity from multiple traits. Ecology 91 (1), 299–305.
Laughlin, D.C., 2014. The intrinsic dimensionality of plant traits and its relevance to community assembly. J. Ecol. 102 (1), 186–193.
Lefsky, M.A., Cohen, W.B., Harding, D.J., Parker, G.G., Acker, S.A., Gower, S.T., 2002. Lidar remote sensing of above-ground biomass in three biomes. Glob. Ecol. Biogeogr. 11, 393–399.
Li, X., Strahler, A.H., 1985. Geometric-optical modeling of a conifer forest canopy. IEEE Trans. Geosci. Remote Sens. 23 (5), 705–721.
Li, X.F., Pei, K.Q., Kéry, M., Niklaus, P.A., Schmid, B., 2017. Decomposing functional trait associations in a Chinese subtropical forest. PLoS One 12 (4), e0175727.
Liang, J., Crowther, T.W., Picard, N., Wiser, S., Zhou, M., Alberti, G., et al., 2016. Positive biodiversity-productivity relationship predominant in global forests. Science 354 (6309), aaf8957.
Liu, X., Swenson, N.G., Lin, D., Mi, X., Umaña, M.N., Schmid, B., et al., 2016. Linking individual-level functional traits to tree growth in a subtropical forest. Ecology 97 (9), 2396–2405.

Liu, X., Trogisch, S., He, J.-S., Niklaus, P.A., Bruelheide, H., Tang, Z., et al., 2018. Tree species richness increases ecosystem carbon storage in subtropical forests. Proc. R. Soc. B 285 (1885), 20181240.
Liu, Y., Sun, D., Hu, X., Ye, X., Li, Y., Liu, S., et al., 2019. The advanced hyperspectral imager: aboard China's GaoFen-5 satellite. IEEE Geosci. Remote Sens. Mag. 7, 23–32.
Ma, X., Mahecha, M.D., Migliavacca, M., van der Plas, F., Benavides, R., Ratcliffe, S., et al., 2019. Inferring plant functional diversity from space: the potential of Sentinel-2. Remote Sens. Environ. 233, 111368.
Ma, X., Migliavacca, M., Wirth, C., Bohn, F.J., Huth, A., Richter, R., et al., 2020. Monitoring plant functional diversity using the reflectance and echo from space. Remote Sens. 12, 1248.
MacArthur, R.H., MacArthur, J.W., 1961. On bird species diversity. Ecology 42 (3), 594–598.
Magurran, A.E., 2004. Measuring Biological Diversity. Blackwell Publishing, Oxford.
Malenovský, Z., Homolová, L., Zurita-Milla, R., Lukeš, P., Kaplan, V., Hanuš, J., et al., 2013. Retrieval of spruce leaf chlorophyll content from airborne image data using continuum removal and radiative transfer. Remote Sens. Environ. 131, 85–102.
Malenovský, Z., Homolová, L., Lukeš, P., Buddenbaum, M., Verrelst, J., Alonso, L., et al., 2019. Variability and uncertainty challenges in scaling imaging spectroscopy retrievals and validations from leaves up to vegetation canopies. Surv. Geophys. 40, 631–656.
Marconi, S., Graves, S.J., Gong, D., Nia, M.S., Le Bras, M., Dorr, B.J., et al., 2019a. A data science challenge for converting airborne remote sensing data into ecological information. PeerJ 6, e5843.
Marconi, S., Graves, S.J., Weinstein, B.G., Bohlman, S.A., White, E.P., 2019b. Estimating individual level plant traits at scale. bioRxiv 556472.
Martin, R.E., Asner, G.P., Sack, L., 2007. Genetic variation in leaf pigment, optical and photosynthetic function among diverse phenotypes of *Metrosideros polymorpha* grown in a common garden. Oecologia 151 (3), 387–400.
Martin, R.E., Chadwick, K.D., Brodrick, P.G., Carranza-Jimenez, L., Vaughn, N.R., Asner, G.P., 2018. An approach for foliar trait retrieval from airborne imaging spectroscopy of tropical forests. Remote Sens. 10 (2), 199.
Mason, N., Mouillot, D., 2013. Functional diversity measures. In: Levin, S.A. (Ed.), Encyclopedia of Biodiversity, Second edition. Academic Press, Waltham, pp. 597–608.
Mason, N.W.H., Mouillot, D., Lee, W.G., Wilson, J.B., 2005. Functional richness, functional evenness and functional divergence: the primary components of functional diversity. Oikos 111 (1), 112–118.
McGill, B.J., Enquist, B.J., Weiher, E., Westoby, M., 2006. Rebuilding community ecology from functional traits. Trends Ecol. Evol. 21, 178–185.
Mendes, G., Arroyo-Rodríguez, V., Almeida, W.R., Pinto, S.R.R., Pillar, V.D., Tabarelli, M., 2015. Plant trait distribution and the spatial reorganization of tree assemblages in a fragmented tropical forest landscape. Plant Ecol. 217, 31–42.
Messier, J., McGill, B.J., Enquist, B.J., Lechowicz, M.J., 2017. Trait variation and integration across scales: is the leaf economic spectrum present at local scales? Ecography 40 (6), 685–697.
Milani, G., Kneubühler, M., Tonolla, D., Doering, M., Wiesenberg, G.L.B., Schaepman, M. E., 2019. Remotely sensing variation in ecological strategies and plant traits of willows in perialpine floodplains. J. Geophys. Res.-Biogeo. 124, 2090–2106.
Moles, A.T., Warton, D.I., Warman, L., Swenson, N.G., Laffan, S.W., Zanne, A.E., et al., 2009. Global patterns in plant height. J. Ecol. 97, 923–932.
Moore, P.T., Van Miegroet, H., Nicholas, N.S., 2007. Relative role of understory and overstory in carbon and nitrogen cycling in a southern Appalachian spruce-fir forest. Can. J. For. Res. 37, 2689–2700.
Morsdorf, F., Meier, E., Kötz, B., Itten, K.I., Dobbertin, M., Allgöwer, B., 2004. Lidar-based geometric reconstruction of boreal type forest stands at single tree level for forest and wildland fire management. Remote Sens. Environ. 92 (3), 353–362.
Morsdorf, F., Kükenbrink, D., Schneider, F.D., Abegg, M., Schaepman, M.E., 2018. Close-range laser scanning in forests: towards physically based semantics across scales. Interface Focus 8, 20170046.
Mouchet, M.A., Villéger, S., Mason, N.W.H., Mouillot, D., 2010. Functional diversity measures: an overview of their redundancy and their ability to discriminate community assembly rules. Funct. Ecol. 24, 867–876.
Myers, N., Mittermeier, R.A., Mittermeier, C.G., da Fonseca, G.A.B., Kent, J., 2000. Biodiversity hotspots for conservation priorities. Nature 403, 853.
Nagendra, H., Rocchini, D., 2008. High resolution satellite imagery for tropical biodiversity studies: the devil is in the detail. Biodivers. Conserv. 17 (14), 3431.
Návar, J., 2019. Modeling tree diversity, stand structure and productivity of northern temperate coniferous forests of Mexico. PeerJ 7, e7051.
Nevalainen, O., Hakala, T., Suomalainen, J., Mäkipää, R., Peltoniemi, M., Krooks, A., et al., 2014. Fast and non-destructive method for leaf level chlorophyll estimation using hyperspectral LiDAR. Agric. For. Meteorol. 198, 250–258.
Noordermeer, L., Bollandsås, O.M., Ørka, H.O., Næsset, E., Gobakken, T., 2019. Comparing the accuracies of forest attributes predicted from airborne laser scanning and digital aerial photogrammetry in operational forest inventories. Remote Sens. Environ. 226, 26–37.
Noss, R.F., 1990. Indicators for monitoring biodiversity: a hierarchical approach. Conserv. Biol. 4, 355–364.
Ollinger, S.V., 2011. Sources of variability in canopy reflectance and the convergent properties of plants. New Phytol. 189, 375–394.
Ørka, H.O., Næsset, E., Bollandsås, O.M., 2009. Classifying species of individual trees by intensity and structure features derived from airborne laser scanner data. Remote Sens. Environ. 113, 1163–1174.
Ørka, H.O., Næsset, E., Bollandsås, O.M., 2010. Effects of different sensors and leaf-on and leaf-off canopy conditions on echo distributions and individual tree properties derived from airborne laser scanning. Remote Sens. Environ. 114 (7), 1445–1461.
Osnas, J.L.D., Katabuchi, M., Kitajima, K., Wright, S.J., Reich, P.B., Van Bael, S.A., et al., 2018. Divergent drivers of leaf trait variation within species, among species, and among functional groups. Proc. Natl. Acad. Sci. 115, 5480–5485.
Ouyang, S., Xiang, W., Wang, X., Xiao, W., Chen, L., Li, S., et al., 2019. Effects of stand age, richness and density on productivity in subtropical forests in China. J. Ecol. 107, 2266–2277.
Paine, C.E.T., Baraloto, C., Chave, J., Hérault, B., 2011. Functional traits of individual trees reveal ecological constraints on community assembly in tropical rain forests. Oikos 120 (5), 720–727.
Paquette, A., Messier, C., 2011. The effect of biodiversity on tree productivity: from temperate to boreal forests. Glob. Ecol. Biogeogr. 20, 170–180.
Pei, Y., Huang, J., Wang, L., Chi, H., Zhao, Y., 2018. An improved phenology-based CASA model for estimating net primary production of forest in Central China based on Landsat images. Int. J. Remote Sens. 39 (21), 7664–7692.
Peintinger, M., Bergamini, A., Schmid, B., 2003. Species–area relationships and nestedness of four taxonomic groups in fragmented wetlands. Basic Appl. Ecol. 4, 385–394.
Petchey, O.L., Gaston, K., 2002. Functional diversity (FD), species richness and community composition. Ecol. Lett. 5, 402–411.
Petchey, O.L., Gaston, K., 2006. Functional diversity: back to basics and looking forward. Ecol. Lett. 9, 741–758.
Pommerening, A., Grabarnik, P., 2019. Theories and Concepts in Individual-Based Forest Ecology, in: Individual-based Methods in Forest Ecology and Management. Springer, Cham, pp. 21–49.
Popescu, S.C., Wynne, R.H., 2004. Seeing the trees in the forest: using lidar and multispectral data fusion with local filtering and variable window size for estimating tree height. Photogramm. Eng. Remote. Sens. 70, 589–604.
Pretzsch, H., Biber, P., 2005. A re-evaluation of Reineke's rule and stand density index. For. Sci. 51 (4), 305–320.
Pretzsch, H., Biber, P., 2016. Tree species mixing can increase maximum stand density. Can. J. For. Res. 46 (10), 1179–1193.
Pretzsch, H., del Río, M., Ammer, C., Avdagic, A., Barbeito, I., Bielak, K., et al., 2015. Growth and yield of mixed versus pure stands of Scots pine (*Pinus sylvestris* L.) and European beech (*Fagus sylvatica* L.) analysed along a productivity gradient through Europe. Eur. J. Forest Res. 134 (5), 927–947.
Reich, P.B., 2005. Global biogeography of plant chemistry: filling in the blanks. New Phytol. 168, 263–268.
Reich, P.B., 2012. Key canopy traits drive forest productivity. Proc. R. Soc. B 279 (1736), 2128–2134.
Richardson, J.J., Moskal, L.M., Kim, S.H., 2009. Modeling approaches to estimate effective leaf area index from aerial discrete-return LIDAR. Agric. For. Meteorol. 149, 1152–1160.
Ruiz-Benito, P., Gómez-Aparicio, L., Paquette, A., Messier, C., Kattge, J., Zavala, M., 2014. Diversity increases carbon storage and tree productivity in Spanish forests. Glob. Ecol. Biogeogr. 23, 311–322.
Sakschewski, B., von Bloh, W., Boit, A., Rammig, A., Kattge, J., Poorter, L., et al., 2015. Leaf and stem economics spectra drive diversity of functional plant traits in a dynamic global vegetation model. Glob. Chang. Biol. 21 (7), 2711–2725.
Salles, J.F., Poly, F., Schmid, B., Roux, X.L., 2009. Community niche predicts the functioning of denitrifying bacterial assemblages. Ecology 90, 3324–3332.
Schaepman, M.E., Ustin, S.L., Plaza, A.J., Painter, T.H., Verrelst, J., Liang, S., 2009. Earth system science related imaging spectroscopy—an assessment. Remote Sens. Environ. 113, S123–S137.
Schaepman, M.E., Jehle, M., Hueni, A., D'Odorico, P., Damm, A., Weyermann, J., et al., 2015. Advanced radiometry measurements and Earth science applications with the Airborne Prism Experiment (APEX). Remote Sens. Environ. 158, 207–219.
Schimel, D., Schneider, F.D., JPL Carbon and Ecosystem Participants, 2019. Flux tower in the sky: global ecology from space. New Phytol. 224, 570–584.
Schleuter, D., Daufresne, M., Massol, F., Argillier, C., 2010. A user's guide to functional diversity indices. Ecol. Monogr. 80, 469–484.
Schmidtlein, S., Feilhauer, H., Bruelheide, H., 2012. Mapping plant strategy types using remote sensing. J. Veg. Sci. 23, 395–405.
Schneider, F.D., Leiterer, R., Morsdorf, F., Gastellu-Etchegorry, J.-P., Lauret, N., Pfeifer, N., et al., 2014. Simulating imaging spectrometer data: 3D forest modeling based on LiDAR and in situ data. Remote Sens. Environ. 152, 235–250.
Schneider, F.D., Morsdorf, F., Schmid, B., Petchey, O.L., Hueni, A., Schimel, D.S., et al., 2017. Mapping functional diversity from remotely sensed morphological and physiological forest traits. Nat. Commun. 8, 1441.
Schneider, F.D., Ferraz, A., Schimel, D., 2019. Watching Earth's interconnected systems at work. Eos 100. https://doi.org/10.1029/2019EO136205.
Schneider, F.D., Ferraz, A.A., Hancock, S., Duncanson, L.I., Dubayah, R.O., Pavlick, R.P., et al., 2020. Towards mapping the diversity of canopy structure from space with GEDI. Environ. Res. Lett. https://doi.org/10.1088/1748-9326/ab9e99 in press.
Schweiger, A.K., Cavender-Bares, J., Townsend, P.A., Hobbie, S.E., Madritch, M.D., Kothari, S., et al., 2020. Spectral niches reveal taxonomic identity and complementarity in plant communities. bioRxiv. https://doi.org/10.1101/2020.04.24.060483.
Seidel, D., Ehbrecht, M., Dorji, Y., Jambay, J., Ammer, C., Annjghöfer, P., 2019. Identifying architectural characteristics that determine tree structural complexity. Trees 33, 911–919.
Serbin, S.P., Singh, A., McNeil, B.E., Kingdon, C.C., Townsend, P.A., 2014. Spectroscopic determination of leaf morphological and biochemical traits for northern temperate and boreal tree species. Ecol. Appl. 24 (7), 1651–1669.

Serbin, S.P., Singh, A., Desai, A.R., Dubois, S.G., Jablonski, A.D., Kingdon, C.C., et al., 2015. Remotely estimating photosynthetic capacity, and its response to temperature, in vegetation canopies using imaging spectroscopy. Remote Sens. Environ. 167, 78–87.
Serrano, L., Peñuelas, J., Ustin, S.L., 2002. Remote sensing of nitrogen and lignin in Mediterranean vegetation from AVIRIS data: decomposing biochemical from structural signals. Remote Sens. Environ. 81 (2), 355–364.
Shen, Z.H., Hu, H.F., Zhou, Y., Fang, J.Y., 2004. Altitudinal patterns of plant species diversity on the southern slope of Mt. Shennongjia, Hubei, China (in Chinese). Biodivers. Sci. 12 (1), 99–107.
Simonson, W.D., Allen, H.D., Coomes, D.A., 2012. Use of an airborne lidar system to model plant species composition and diversity of Mediterranean oak forests. Conserv. Biol. 26 (5), 840–850.
Singh, A., Serbin, S.P., McNeil, B.E., Kingdon, C.C., Townsend, P.A., 2015. Imaging spectroscopy algorithms for mapping canopy foliar chemical and morphological traits and their uncertainties. Ecol. Appl. 25 (8), 2180–2197.
Smith, A.B., Sandel, B., Kraft, N.J.B., Carey, S., 2013. Characterizing scale-dependent community assembly using the functional-diversity–area relationship. Ecology 94, 2392–2402.
Spasojevic, M.J., Suding, K.N., 2012. Inferring community assembly mechanisms from functional diversity patterns: the importance of multiple assembly processes. J. Ecol. 100, 652–661.
Swenson, N.G., Weiser, M.D., 2010. Plant geography upon the basis of functional traits: an example from eastern North American trees. Ecology 91, 2234–2241.
Swenson, N.G., Enquist, B.J., Pither, J., Kerkhoff, A.J., Boyle, B., Weiser, M.D., et al., 2012. The biogeography and filtering of woody plant functional diversity in North and South America. Glob. Ecol. Biogeogr. 21 (8), 798–808.
Thonicke, K., Billing, M., von Bloh, W., Sakschewski, B., Niinemets, Ü., Peñuelas, J., et al., 2020. Simulating functional diversity of European natural forests along climatic gradients. J. Biogeogr. 47, 1069–1085.
Tian, Z., Chen, Y., Chen, W., Hu, D., 2002. Vegetation mapping and analysis at Longmenhe region, Shennongjia, China (in Chinese). Acta Phytoecol. Sin. 26 (Suppl), 30–39.
Umaña, M.N., Swenson, N.G., 2019. Does trait variation within broadly distributed species mirror patterns across species? A case study in Puerto Rico. Ecology 100 (8), e02745.
UNESCO World Heritage Centre, 2016. World Heritage List: Hubei Shennongjia. https://whc.unesco.org/en/list/1509/ (accessed 30 April 2020).
Ustin, S.L., Gamon, J.A., 2010. Remote sensing of plant functional types. New Phytol. 186, 795–816.
Ustin, S.L., Gitelson, A.A., Jacquemoud, S., Schaepman, M., Asner, G.P., Gamon, J.A., et al., 2009. Retrieval of foliar information about plant pigment systems from high resolution spectroscopy. Remote Sens. Environ. 113, S67–S77.
Valbuena, R., O'Connor, B., Zellweger, F., Simonson, W., Vihervaara, P., Maltamo, M., et al., 2020. Standardising ecosystem morphological traits from 3D information sources. Trends Ecol. Evol. 35 (8), 656–667.
Verrelst, J., Camps-Valls, G., Muñoz-Marí, J., Rivera, J.P., Veroustraete, F., Clevers, J.G. P.W., et al., 2015. Optical remote sensing and the retrieval of terrestrial vegetation bio-geophysical properties – a review. ISPRS J. Photogramm. Remote Sens. 108, 273–290.
Verrelst, J., Malenovský, Z., van der Tol, C., Camps-Valls, G., Gastellu-Etchegorry, J.P., Lewis, P., et al., 2019. Quantifying vegetation biophysical variables from imaging spectroscopy data: a review on retrieval methods. Surv. Geophys. 40, 589–629.
Villéger, S., Mason, N.W.H., Mouillot, D., 2008. New multidimensional functional diversity indices for a multifaceted framework in functional ecology. Ecology 89 (8), 2290–2301.
Violle, C., Navas, M.-L., Vile, D., Kazakou, E., Fortunel, C., Hummel, I., et al., 2007. Let the concept of trait be functional! Oikos 116, 882–892.
Violle, C., Reich, P.B., Pacala, S.W., Enquist, B.J., Kattge, J., 2014. The emergence and promise of functional biogeography. Proc. Natl. Acad. Sci. 111, 13690–13696.
Walker, B.H., 1992. Biodiversity and ecological redundancy. Conserv. Biol. 6, 18–23.
Wang, R., Gamon, J., 2019. Remote sensing of terrestrial plant biodiversity. Remote Sens. Environ. 231, 111218.
Wang, Y., Hyyppä, J., Liang, X., Kaartinen, H., Yu, X., Lindberg, E., et al., 2016a. International benchmarking of the individual tree detection methods for modeling 3-D canopy structure for silviculture and forest ecology using airborne laser scanning. IEEE Trans. Geosci. Remote Sens. 54 (9), 5011–5027.
Wang, Z., Wang, T., Darvishzadeh, R., Skidmore, A., Jones, S., Suarez, L., et al., 2016b. Vegetation indices for mapping canopy foliar nitrogen in a mixed temperate forest. Remote Sens. 8, 491.
Wang, Z., Chlus, A., Geygan, R., Ye, Z., Zheng, T., Singh, A., et al., 2020. Foliar functional traits from imaging spectroscopy across biomes in eastern North America. New Phytol. 228, 494–511.
Westoby, M., 1998. A leaf-height-seed (LHS) plant ecology strategy scheme. Plant Soil 199 (2), 213–227.
Williams, L.J., Paquette, A., Cavender-Bares, J., Messier, C., Reich, P.B., 2017. Spatial complementarity in tree crowns explains overyielding in species mixtures. Nat. Ecol. Evol. 1, 0063.
Wills, C., Condit, R., Foster, R.B., Hubbell, S.P., 1997. Strong density- and diversity-related effects help to maintain tree species diversity in a neotropical forest. Proc. Natl. Acad. Sci. 94 (4), 1252–1257.
Wright, I.J., Reich, P.B., Westoby, M., Ackerly, D.D., Baruch, Z., Bongers, F., et al., 2004. The world-wide leaf economics spectrum. Nature 428, 821–827.
Xu, W., Ge, J., Xiong, G., Zhao, C., Shen, G., Fan, D., et al., 2017. A dataset of species composition in a typical subtropical mixed evergreen and deciduous broad-leaved forest (2001). China Sci. Data 2 (1), 66–71.
Yang, J., Cao, M., Swenson, N.G., 2018. Why functional traits do not predict tree demographic rates. Trends Ecol. Evol. 33 (5), 326–336.
Zarco-Tejada, P.J., Miller, J.R., Noland, T.L., Mohammed, G.H., Sampson, P.H., 2001. Scaling-up and model inversion methods with narrowband optical indices for chlorophyll content estimation in closed forest canopies with hyperspectral data. IEEE Trans. Geosci. Remote Sens. 39, 1491–1507.
Zeng, Y., Huang, J.X., Wu, B.F., Schaepman, M.E., de Bruin, S., Clevers, J.G.P.W., 2008a. Comparison of the inversion of two canopy reflectance models for mapping forest crown closure using imaging spectroscopy. Can. J. Remote. Sens. 34, 235–244.
Zeng, Y., Schaepman, M.E., Wu, B., Clevers, J.G.P.W., Bregt, A.K., 2008b. Scaling-based forest structural change detection using an inverted geometric-optical model in the Three Gorges region of China. Remote Sens. Environ. 112 (12), 4261–4271.
Zeng, Y., Schaepman, M.E., Wu, B., Clevers, J.G.P.W., Bregt, A.K., 2009. Quantitative forest canopy structure assessment using an inverted geometric-optical model and up-scaling. Int. J. Remote Sens. 30 (6), 1385–1406.
Zhao, C., Chen, W., Tian, Z., Xie, Z., 2005. Altitudinal pattern of plant species diversity in Shennongjia Mountains, Central China. J. Integr. Plant Biol. 47 (12), 1431–1449.
Zhao, D., Pang, Y., Li, Z., Sun, G., 2013. Filling invalid values in a Lidar-derived canopy height model with morphological crown control. Int. J. Remote Sens. 34, 4636–4654.
Zhao, D., Pang, Y., Li, Z., Liu, L., 2014. Isolating individual trees in a closed coniferous forest using small footprint Lidar data. Int. J. Remote Sens. 35, 7199–7218.
Zhao, Y., Zeng, Y., Zhao, D., Wu, B., Zhao, Q., 2016. The optimal leaf biochemical selection for mapping species diversity based on imaging spectroscopy. Remote Sens. 8 (3), 216.
Zhao, Y., Zeng, Y., Zheng, Z., Dong, W., Zhao, D., Wu, B., et al., 2018. Forest species diversity mapping using airborne LiDAR and hyperspectral data in a subtropical forest in China. Remote Sens. Environ. 213, 104–114.